Griffith UNIVERSITY
Griffith Business School
Queensland, Australia

A penalization approach for estimating inefficiency in stochastic frontier panel models

Firmin Doko Tchatoka* Magnus Söderberg † Mohammad Abbas Hakeem‡

January 21, 2025

Abstract

Efficiency analysis is crucial for evaluating the performance of entities that provide essential and other homogenized services. The Jondow et al.'s (1982) estimator is widely used but has been criticized for biasing inefficiency toward its mean, distorting the distribution, and misrepresenting the conditional distribution of inefficiency, particularly in cross-sectional settings. Zeebari et al. (2023) propose a regularization approach that aligns sample and theoretical moments but it is primarily suited to cross-sectional data. This paper introduces a penalized mode estimator for unit inefficiency in panel data, accounting for heteroskedasticity in both inefficiency and idiosyncratic errors. A closed-form expression for this estimator is derived, and Monte Carlo simulations demonstrate its superior performance compared to existing methods. An empirical study of electricity providers in Australia, Canada, and New Zealand further underscores its advantages.

Key words: Inefficiency, Stochastic frontier panel model, JLMS estimator, Heteroskedasticity, Restricted mode estimator.

JEL classi ication: C13, C23, C16, H21

*Corresponding author contacts: School of Economics and Public Policy, The University of Adelaide, 10 Pulteney St, Adelaide SA 5005, AUSTRALIA. E-mail: firmin.dokotchatoka@adelaide.edu.au

†Centre of Applied Energy Economics and Policy Research, Griffith University, Parklands Drive, Southport QLD 4222, Australia. E-mail: m.soderberg@griffith.edu.au

‡School of Economics and Public Policy, The University of Adelaide, 10 Pulteney St, Adelaide SA 5005, AUSTRALIA. E-mail: abbas.hakeem@adelaide.edu.au

1 Introduction

Stochastic Frontier Analysis (SFA) is a widely used framework for evaluating the performance and productivity of entities that provide homogenized services.[1] Given their frequent local monopoly status, the performance of essential services is often assessed through SFA (see e.g. Price et al., 2017; Söderberg, 2008; Piacenza, 2006). SFA identifies the efficient frontier, which represents the maximum achievable output for a given set of inputs, and treats deviations from the frontier as technical inefficiencies. These deviations are critical for estimating efficiency levels and identifying the sources of inefficiency within production or cost models.

The standard method for estimating inefficiency, introduced by Jondrow et al. (1982) and known as the JLMS estimator, focuses on the conditional mean or mode of inefficiency, given the composite error. Although commonly used in cross-sectional settings, the JLMS estimator has notable limitations. It shrinks inefficiency estimates towards their mean or mode, leading to the underestimation of the most inefficient units and the overestimation of the least inefficient ones (Wang and Schmidt, 2009; Horrace et al., 2023; Zeebari et al., 2023). Furthermore, the conditional distribution of the inefficiency estimated by JLMS often deviates from the true inefficiency distribution, particularly when the inefficiency is estimated based on the composite error rather than its theoretical counterpart (Horrace, 2005; Kumbhakar et al., 2015). These limitations have raised concerns among researchers and regulatory agencies, as inaccurate inefficiency estimation can lead to suboptimal policies, misallocation of resources, and hindered productivity improvements; see, e.g., Badunenko et al. (2012), Stone (2002), Tsionas (2017), and Andor et al. (2019).

To address these concerns, Zeebari et al. (2023) proposed a regularization approach that aligns the sample moments of the composite error with their theoretical counterparts. Although effective in cross-sectional settings, this approach does not account for the complexities inherent in panel data, such as unobserved heterogeneity and temporal dynamics. Panel data models, which incorporate both time and cross-sectional dimensions, offer a more comprehensive framework for understanding efficiency dynamics. They allow for the comparison of efficiency levels across units while accounting for individual-specific and time-specific effects, thereby enhancing the accuracy of inefficiency estimates.

Building on the work of Zeebari et al. (2023), this paper introduces a restricted conditional mode estimator tailored for panel data stochastic frontier models. Our methodology extends the penalized maximum likelihood estimation framework to account for heteroskedasticity in

[1] Examples include healthcare (Lovell, 2006), construction (Nazarko and Chodakowska, 2017), and insurance (Fenn et al., 2008). However, there are also examples of more general applications, using data from a wide range of listed firms (Manzur Quader and Dietrich, 2014).

both inefficiency and idiosyncratic errors, while allowing for weak dependence of inefficiencies over time.

The importance of heteroskedasticity in SFA was first emphasized by Caudill and Ford (1993) and Caudill et al. (1995), and later extended to panel data by Wang (2002), who argued that controlling for heteroskedasticity is essential to correct model misspecifications and better understand the impact of external factors on inefficiency. Similarly, the limitation of overlooking the time-varying nature of inefficiencies has been highlighted by Lawrence et al. (2018), Roberts (2018), and Lee et al. (2021).

We derive closed-form expressions for the estimator of inefficiency under three common distributions. Exponential, half normal, and truncated normal.

Through Monte Carlo simulations, we demonstrate that the proposed restricted-mode estimator significantly outperforms traditional methods, particularly in mitigating shrinkage bias and improving inefficiency estimation for the most inefficient units. An empirical application to electricity Distribution Network Service Providers (DNSPs) in Australia, New Zealand, and Ontario (Canada) highlights the practical advantages of our approach. It reveals that traditional estimators systematically underestimate inefficiency of the most inefficient units, emphasizing the importance of penalization and dynamic modeling for accurate and reliable inefficiency estimates.

Significant contributions to the SFA literature include the fixed effects model developed by Greene (2005a), which differentiates firm-specific heterogeneity from inefficiency using maximum likelihood estimation with dummy variables. However, this model suffers from an incidental parameter problem that affects variance estimates. To address this, Wang and Ho (2010) and Chen et al. (2014) proposed methods to remove fixed effects, but they maintained the assumption of homoskedastic errors. Kumbhakar et al. (2014) highlighted that this assumption is often unrealistic, leading Belotti and Ilardi (2018), among others, to relax it by allowing for conditional heteroskedasticity and dynamic inefficiencies.

Despite these advancements, the existing literature, including Belotti and Ilardi (2018), focuses primarily on the JLMS mean estimator, which suffers from shrinkage bias. As discussed previously, this leads to inaccuracies in estimating inefficiency, particularly for the most and least inefficient units (Zeebari et al., 2023). Our methodology improves upon this by restricting the sample first moment of the idiosyncratic error to match its theoretical counterpart, resulting in a more reliable mode estimator compared to the standard unrestricted mode estimator.

The remainder of this paper is organized as follows. Section 2 introduces the model framework and assumptions, followed by a description of the standard conditional mode estimator

and the derivation of our proposed restricted conditional mode estimator. Section 3 presents the performance of our methods through Monte Carlo simulations. Section 4 illustrates the proposed methodology with an empirical application to the operating cost model of electricity Distribution Network Service Providers in Australia, New Zealand, and Ontario (Canada). Finally, Section 5 concludes.

2 Setup

We consider the panel stochastic frontier (SF) framework of Belotti and Ilardi (2018):[2]

$$y_{it} = \alpha_i + x'_{it}\beta + \varepsilon_{it} \tag{2.1}$$

$$\varepsilon_{it} = v_{it} - u_{it},\ u_{it} \geq 0 \tag{2.2}$$

for all $i = 1, \ldots, n$ and $t = 1, \ldots, T$. Here, y_{it} denotes the logarithm of output for unit i at time t, x_{it} represents a $k \times 1$ vector of exogenous inputs, β is a $k \times 1$ vector of technology parameters, and α_i is the fixed-effect of unit i. The terms v_{it} and u_{it} represent the idiosyncratic and the inefficiency errors, respectively, of unit i at time t. Equation (2.2) encompasses the SF production model. When accounting for the SF cost model, we substitute (2.2) with $\varepsilon_{it} = v_{it} + u_{it}$. However, for our theoretical analysis, we primarily focus on the SF production model while maintaining generality.

Recent literature emphasizes the importance of integrating conditional heteroskedasticity and time variation into the distributions of inefficiency and idiosyncratic shock. In this regard, we assume that

$$v_{it} \overset{iid}{\sim} \mathscr{N}(0, \psi_{it}^2),\ \ u_{it} \overset{iid}{\sim} \mathscr{F}_u(\theta_{it}), \tag{2.3}$$

where ψ_{it} and θ_{it} are functions of exogenous covariates. $\mathscr{F}_u(\theta_{it})$ can follow various forms: an exponential distribution with a scale parameter σ_{it} $[u_{it} \sim \mathscr{E}(\sigma_{it})]$, a half-normal distribution with zero mean and variance $\sigma_{it}^2[u_{it} \sim \mathscr{N}^+(0, \sigma_{it}^2)]$, or a truncated normal distribution with mean ν_{it} and variance σ_{it}^2 $[u_{it} \sim \mathscr{N}^+(\nu_{it}, \sigma_{it}^2)]$. Here, we assume that $\sigma_{it} = g(z_{it}, \gamma)$, $\psi_{it} = h(w_{it}, \delta)$, and $\nu_{it} = q(\tilde{z}_{it}, \tilde{\gamma})$, where $g(\cdot)$ and $h(\cdot)$ are positive monotonic functions, and z_{it}, w_{it}, and $\tilde{z}_{it}$ are vectors of exogenous covariates. The parameters γ, $\tilde{\gamma}$, δ, and β are unknown and will be estimated jointly.

Belotti and Ilardi (2018) develop different methodologies to estimate the conditional mean

[2]For further details, refer to Greene (2005a,b).

of u_{it} in equations (2.1)-(2.3), given the composite error using the JLMS approach. It is widely acknowledged that the JLMS estimator shrinks the inefficiency towards its mean, resulting in a distribution different from the true inefficiency distribution (Wang and Schmidt, 2009). Recent research by Zeebari et al. (2023) established that the conditional mean and mode underestimate the inefficiencies of the most inefficient units. As an alternative, Zeebari et al. (2023) propose regularized conditional model estimators, obtained by constraining the sample moments of idiosyncratic error and inefficiency to match their theoretical counterparts. However, their findings are suitable only for cross-sectional data with homogeneous inefficiency and idiosyncratic errors.

This paper proposes an approach that combines the innovations of Belotti and Ilardi (2018) and Zeebari et al. (2023). Specifically, we introduce a penalized maximum likelihood estimation of the conditional mode estimator for the inefficiency, while simultaneously accounting for time variation and conditional heterogeneity in the inefficiency and idiosyncratic shocks.

2.1 Unrestricted conditional mode estimator of the efficiency

Let $f_u(\cdot;\theta)$ and $f_\varepsilon(\cdot;\theta)$ represent the probability density functions (PDFs) of u_{it} and ε_{it} respectively, where $\theta = (\beta', \gamma', \delta')'$ is the unknown parameter vector of the panel SF model. Let $\{(u_{it}, v_{it}) : i = 1, \ldots, n; t = 1, \ldots, T\}$ be a sample of i.i.d. observations drawn from this SF model. Then, the conditional PDF of u_{it}, given $\varepsilon_{it} = v_{it} - u_{it}$, is

$$f_{u|\varepsilon}(u_{it}) \quad = \quad \frac{f_u(u_{it})\phi(\varepsilon_{it} + u_{it}; \psi_{it}^2)}{f_\varepsilon(\varepsilon_{it})} \tag{2.4}$$

where $\phi(\varepsilon_{it} + u_{it}; \psi_{it}^2)$ is the pdf of $\mathcal{N}(0, \psi_{it}^2)$ evaluated at $v_{it} = \varepsilon_{it} + u_{it}$. Under the i.i.d. assumption of u_{it} over time, we can find the conditional mode estimator at time t by maximizing the conditional likelihood function of the n units obtained from Equation (2.4) with respect to u_{it}, $i = 1, \ldots, n$. That is, the Maximum Likelihood (ML) estimator of the mode of the conditional distribution of u_{it}, given ε_{it}, is $\mathbb{M}(u_{it}|\varepsilon_{it}, \theta) = \max\{0, \mathbf{M}(u_{it}|\varepsilon_{it}, \theta)\}$ where

$$\mathbf{M}(u_{it}|\varepsilon_{it}, \theta) \quad = \quad \underset{u_{1t},\ldots,u_{nt}}{\arg\max} \sum_{i=1}^{n} \Big(ln\big[\phi(\varepsilon_{it} + u_{it}; \psi_{it}^2)\big] + ln\big[f_u(u_{it})\big] \Big) \tag{2.5}$$

for all $t = 1, \ldots, T$. A closed-form solution to the maximization problem in Equation (2.5) can easily be obtained through straightforward calculations, yielding:

$$\mathbf{M}(u_{it}|\varepsilon_{it}, \theta) = -\Big(\frac{\sigma_{it}^2}{\sigma_{it}^2 + \psi_{it}^2}\Big)\varepsilon_{it}.$$

Hence, we can express $\mathbb{M}(u_{it}|\varepsilon_{it},\theta)$ for all $i=1,\ldots,n$ and $t=1,\ldots,T$ as:

$$\mathbb{M}(u_{it}|\varepsilon_{it},\theta) \quad = \quad -\Big(\frac{\sigma_{it}^2}{\sigma_{it}^2+\psi_{it}^2}\Big)\varepsilon_{it}\mathbb{1}(\varepsilon_{it}\leq 0). \tag{2.6}$$

Note that in Equation (2.6) the ML estimator $\mathbb{M}(u_{it}|\varepsilon_{it},\theta)$ depends on the unknown parameter vector θ, rendering it an infeasible estimator. Suppose a consistent estimator $\hat{\theta}$ of θ is available. Then, a point estimate of the mode of the conditional distribution of the inefficiency is obtained by substituting ε_{it} and θ with their estimates $\hat{\varepsilon}_{it}$ and $\hat{\theta}$ in Equation (2.6). Specifically,

$$\mathbb{M}(u_{it}|\hat{\varepsilon}_{it},\hat{\theta}) = -\Big(\frac{\hat{\sigma}_{it}^2}{\hat{\sigma}_{it}^2+\hat{\psi}_{it}^2}\Big)\hat{\varepsilon}_{it}\mathbb{1}(\hat{\varepsilon}_{it}\leq 0). \tag{2.7}$$

We also provide the analytical expressions of $\mathbb{M}(u_{it}|\hat{\varepsilon}it,\hat{\theta})$ when $u_{it}\sim\mathscr{E}(\sigma_{it})$ (exponential with scale parameter σ_{it}) and $u_{it}\sim\mathscr{N}^{+}(\nu_{it},\sigma_{it}^2)$ (truncated normal with mean ν_{it} and variance σ_{it}^2), as shown in Equation (2.8):

$$\mathbb{M}(u_{it}|\hat{\varepsilon}_{it},\hat{\theta}) = \begin{cases} -\Big(\hat{\varepsilon}_{it}+\frac{\hat{\psi}_{it}^2}{\hat{\sigma}_{it}}\Big)\mathbb{1}(\hat{\varepsilon}_{it}\leq 0) & \text{if } u_{it}\sim\mathscr{E}(\sigma_{it}) \\ \\ -\Big(\frac{\hat{\sigma}_{it}^2\hat{\varepsilon}_{it}}{\hat{\sigma}_{it}^2+\hat{\psi}_{it}^2}-\frac{\hat{\psi}_{it}^2\hat{\nu}_{it}}{\hat{\sigma}_{it}^2+\hat{\psi}_{it}^2}\Big)\mathbb{1}(\hat{\varepsilon}_{it}\leq 0) & \text{if } u_{it}\sim\mathscr{N}^{+}(\nu_{it},\sigma_{it}^2). \end{cases} \tag{2.8}$$

Remark 1. $\mathbb{M}(u_{it}|\hat{\varepsilon}_{it},\hat{\theta})$ is an MLE, thus is appealing compared with the the JLMS conditional mean estimator. However, $\mathbb{M}(u_{it}|\hat{\varepsilon}_{it},\hat{\theta})$ does not measure the unconditional inefficiency u_{it} itself but rather a characteristic of its distribution (see e.g., Kumbhakar et al., 2020).

Remark 2. $\mathbb{M}(u_{it}|\hat{\varepsilon}_{it},\hat{\theta})$ captures the unconditional inefficiency solely in the absence of idiosyncratic error (i.e., when $v_{it}=0$); see e.g. Zeebari et al. (2023). In the context of homoskedastic errors within the cross-sectional framework, Zeebari et al. (2023) propose alternative restricted mode estimators, which do not incorporate time variation in the inefficiency and idiosyncratic error distributions. In Section 2.2, we introduce a penalized maximum likelihood approach that accounts for time variation and conditional heteroskedasticity in the inefficiency and idiosyncratic error distributions.

2.2 Penalized maximum likelihood mode estimator of the inefficiency

For simplicity and without any loss of generality, we assume that the functions $g(\cdot)$, $h(\cdot)$, and $q(\cdot)$ in (2.3) are defined as:

$$\sigma_{it} = \exp(\gamma_0 + z_{it}'\gamma_1), \quad \psi_{it} = \exp(\delta_0 + w_{it}'\delta_1), \quad \text{and} \quad \nu_{it} = \tilde{\gamma}_0 + \tilde{z}_{it}'\tilde{\gamma}_1,$$

for some exogenous covariates z_{it}, w_{it}, and $\tilde{z}_{it}$. Here, $\gamma = (\gamma_0, \gamma_1')'$, $\delta = (\delta_0, \delta_1')'$, and $\tilde{\gamma} = (\tilde{\gamma}_0, \tilde{\gamma}_1')'$ represent unknown parameter vectors that determine the conditional distribution of the efficiency. When $\gamma_1 = 0$ and $\delta_1 = 0$, it follows that $\sigma_{it}^2 = \sigma^2$ and $\psi_{it}^2 = \psi^2$ for all i and t. Consequently, the hypothesis of conditional homoskedasticity in the variance of u_{it} (or v_{it}) can be tested by evaluating the null hypothesis $\gamma_1 = 0$ (or $\delta_1 = 0$) within the framework of this stochastic frontier panel model.

Our focus is on estimating the conditional mode of unit inefficiency u_{it} while restricting the sample mean of the idiosyncratic error v_{it} to zero. Let $(\varepsilon_{it})_{i=1}^n$ denote a sample of observations on the composite error across units at time t, and define $\theta = (\gamma', \delta', \tilde{\gamma}')'$. The penalized maximum likelihood mode estimator of u_{it}, subject to the constraint that the sample average of the idiosyncratic error is zero, conditioned on $(\varepsilon_{it})_{i=1}^n$, is expressed as:

$$\mathbb{M}_r(u_{it}|\varepsilon_{it}, \theta) = \max\left\{0, \tilde{u}_{it}(\varepsilon_{it}, \theta)\right\}, \tag{2.9}$$

where $\tilde{u}_{it}(\varepsilon_{it}, \theta)$ solves

$$\begin{aligned} &\max_{u_{1t},\ldots,u_{nt}} \sum_{i=1}^{n} \Big(ln\big[\phi(\varepsilon_{it} + u_{it}; \psi_{it}^2)\big] + ln\big[f_u(u_{it})\big] \Big) \\ &s.t. \sum_{i=1}^{n} v_{it} = \sum_{i=1}^{n} (\varepsilon_{it} + u_{it}) = 0, \quad t = 1, \ldots, T. \end{aligned} \tag{2.10}$$

We can express this optimization problem as: $\max_{u_{1t},\ldots,u_{nt},\lambda_t} \mathscr{L}(u_{1t}, \ldots, u_{nt}, \lambda_t; \theta)$, where

$$\mathscr{L}(u_{1t}, \ldots, u_{nt}, \lambda_t; \theta) = \sum_{i=1}^{n} \Big(ln\big[\phi(\varepsilon_{it} + u_{it}; \psi_{it}^2)\big] + ln\big[f_u(u_{it})\big] \Big) + \lambda_t \sum_{i=1}^{n} (\varepsilon_{it} + u_{it}), \tag{2.11}$$

with λ_t denoting the Lagrange multiplier which may vary over time.

The explicit form of the penalized conditional mode estimator of unit inefficiencies is presented in Theorem 2.1 for three cases: (i) when u_{it} follows a half-normal distribution with zero mean and variance σ_{it}^2, (ii) when u_{it} follows an exponential distribution with scale parameter σ_{it}, and (iii) when u_{it} follows a truncated normal distribution with mean ν_{it} and variance σ_{it}^2. It should be noted that the latter two distributional settings imply that both the mean and variance of the inefficiency vary between units and over time.

Theorem 2.1 *Suppose Equations (2.1)-(2.2) are satisfied, with v_{it} following an i.i.d. normal*

distribution $\mathscr{N}(0,\psi_{it}^2)$ *and* u_{it} *following an i.i.d. distribution* $\mathscr{F}_u$. *In this scenario, the regularized mode estimator of the conditional distribution of* u_{it} *is expressed as* $\mathbb{M}_r(u_{it}|\varepsilon_{it},\theta) = \max\{0,\tilde{u}_{it}(\varepsilon_{it},\theta)\}$, *where the explicit form of* $\tilde{u}_{it}(\varepsilon_{it},\theta)$ *is presented below:*

(*a*) *If* $u_{it} \sim \mathscr{F}_u \equiv \mathscr{N}^+(0,\sigma_{it}^2)$, *then*

$$\tilde{u}_{it}(\varepsilon_{it},\theta) \;=\; -\Big(\frac{\sigma_{it}^2}{\sigma_{it}^2+\psi_{it}^2}\Big)\varepsilon_{it} - \Big(\frac{\sigma_{it}^2\psi_{it}^2}{(\sigma_{it}^2+\psi_{it}^2)(\bar{\psi}_t^2-\bar{\eta}_t)}\Big)\bar{\varepsilon}_t^*,\; i=1,\ldots,n, \tag{2.12}$$

where $\bar{\psi}_t^2 = \frac{1}{n}\sum_{i=1}^n \psi_{it}^2$, $\bar{\eta}_t = \frac{1}{n}\sum_{i=1}^n \big(\frac{\psi_{it}^4}{\sigma_{it}^2+\psi_{it}^2}\big)$ *and* $\bar{\varepsilon}_t^* = \frac{1}{n}\sum_{i=1}^n \big(\frac{\psi_{it}^2}{\sigma_{it}^2+\psi_{it}^2}\big)\varepsilon_{it}$;

(*b*) *If* $u_{it} \sim \mathscr{F}_u \equiv \mathscr{F}_u(\sigma_{it}) \equiv \mathscr{E}(\sigma_{it})$, *then*

$$\tilde{u}_{it}(\varepsilon_{it},\theta) \;=\; -\varepsilon_{it} + \Big(\frac{\psi_{it}^2}{\bar{\psi}_t^2}\Big)\bar{\zeta}_t - \frac{\psi_{it}^2}{\sigma_{it}},\; i=1,\ldots,n, \tag{2.13}$$

where $\bar{\zeta}_t = \frac{1}{n}\sum_{i=1}^n \big(\frac{\psi_{it}^2}{\sigma_{it}}\big)$ *and* $\bar{\psi}_t^2$ *is given in* (*a*);

(*c*) *If* $u_{it} \overset{i.i.d.}{\sim} \mathscr{F}_u \equiv \mathscr{N}^+(\nu_{it},\sigma_{it}^2)$, *then*

$$\begin{aligned}\tilde{u}_{it}(\varepsilon_{it},\theta) \;=\; & -\Big(\frac{\sigma_{it}^2}{\sigma_{it}^2+\psi_{it}^2}\Big)\varepsilon_{it} - \Big(\frac{\sigma_{it}^2\psi_{it}^2}{(\sigma_{it}^2+\psi_{it}^2)(\bar{\psi}_t^2-\bar{\eta}_t)}\Big)\bar{\varepsilon}_t^* + \\ & -\frac{\sigma_{it}^2\psi_{it}^2}{(\sigma_{it}^2+\psi_{it}^2)(\bar{\psi}_t^2-\bar{\eta}_t)}\left[\frac{\bar{\omega}_t^2\bar{\eta}_t}{\bar{\psi}_t^2} + \frac{(\bar{\psi}_t^2-\bar{\eta}_t)\bar{\omega}_t^2}{\bar{\psi}_t^2} - \frac{(\bar{\psi}_t^2-\bar{\eta}_t)}{\sigma_{it}^2} - \bar{\kappa}_t\right]\nu_{it} \\ & \textit{for all } i=1,\ldots,n,\end{aligned} \tag{2.14}$$

where $\bar{\psi}_t^2$, $\bar{\eta}_t$ *and* $\bar{\varepsilon}_t^*$ *are defined in* (*a*), $\bar{\omega}_t^2 = \frac{1}{n}\sum_{i=1}^n \big(\frac{\psi_{it}^2}{\sigma_{it}^2}\big)$ *and* $\bar{\kappa}_t = \frac{1}{n}\sum_{i=1}^n \big(\frac{\psi_{it}^4}{\sigma_{it}^2(\sigma_{it}^2+\psi_{it}^2)}\big)$.

Some observations are in order.

Remark 1 (Homoskedasticity). If both u_{it} and v_{it} are homoskedastic across i and t, that is, $\sigma_{it}^2 = \sigma^2$ and $\psi_{it}^2 = \psi^2$ for all t and i, then we have $\bar{\psi}_t^2 = \psi^2$, $\bar{\eta}_t = \frac{\psi^4}{\sigma^2+\psi^2}$, $\bar{\zeta}_t = \frac{\psi^2}{\sigma}$ and $\bar{\varepsilon}_t^* = \frac{\psi^2\bar{\varepsilon}}{\sigma^2+\psi^2}$, where $\bar{\varepsilon} = \frac{1}{n}\sum_{i=1}^n \varepsilon_{it}$. Therefore, Equations (2.12)-(2.13) become:

$$\tilde{u}_{it}(\varepsilon_{it},\theta) \;=\; -\Big(\frac{\sigma^2}{\sigma^2+\psi^2}\Big)\varepsilon_{it} - \Big(\frac{\psi^2}{\sigma^2+\psi^2}\Big)\bar{\varepsilon} \tag{2.15}$$

$$\tilde{u}_{it}(\varepsilon_{it},\theta) \;=\; -\varepsilon_{it}, \tag{2.16}$$

which are identical to the cross-sectional estimators of Zeebari et al. (2021) but vary across time and units. Additionally, if $\nu_{it} = \nu$ for all i and t, then Equation (2.14) collapses to

$$\tilde{u}_{it}(\varepsilon_{it},\theta) \;=\; -\Big(\frac{\sigma^2}{\sigma^2+\psi^2}\Big)\varepsilon_{it} - \Big(\frac{\psi^2}{\sigma^2+\psi^2}\Big)\bar{\varepsilon}, \tag{2.17}$$

which again is similar to Zeebari et al.'s (2021) first moment restricted estimator with truncated normal inefficiencies. However, if heteroskedasticity is present (even if it does not vary over time), the regularized mode estimators in Equations (2.12)-(2.14) differ from their homoskedastic counterparts in Equations (2.15)-(2.17). This underscores the significance of accounting for heteroskedasticity, even in the cross-sectional setting.

Remark 2 (Feasible estimator). The penalized estimators in Equations (2.12)-(2.14) are infeasible because they depend on the unobserved composite error ε_{it} and the unknown parameter vector θ. Feasible estimators are obtained by replacing ε_{it} and θ with their estimates $\hat{\varepsilon}_{it}$ and $\hat{\theta}$ as described in Section 2.3. Under the regularity conditions ensuring the consistency of $\hat{\theta}$, $\mathbb{M}_r(u_{it}|\hat{\varepsilon}_{it}, \hat{\theta})$ is a consistent estimator of $\mathbb{M}_r(u_{it}|\varepsilon_{it}, \theta)$.

Remark 3 (Practical implementation). We have developed a user-written *Stata package* that implements the regularized conditional estimator $\mathbb{M}_r(u_{it}|\hat{\varepsilon}_{it}, \hat{\theta})$ for the three sets of inefficiency distributions described in Theorem 2.1. The code implements $\mathbb{M}_r(u_{it}|\hat{\varepsilon}_{it}, \hat{\theta})$ after the PD estimation using the *sftfe command* provided by Belotti et al. (2014). The *sftfe command* expresses the mean and variance of inefficiency, together with the variance of the idiosyncratic error, as functions of exogenous covariates.

2.3 Estimation

One commonly employed approach to achieve consistent estimation of θ in equations (2.1) through (2.3) involves utilizing a first-difference transformation (see e.g. Wang and Ho, 2010; Belotti and Ilardi, 2018) to remove the fixed-effect parameters α_i:

$$\Delta y_i = \Delta X_i'\beta + \Delta\varepsilon_i \tag{2.18}$$

$$\Delta\varepsilon_i = \Delta v_i - \Delta u_i, \tag{2.19}$$

$$\Delta v_i \overset{iid}{\sim} \mathscr{N}_{T-1}(0, \Psi),\ \Delta u_i \overset{iid}{\sim} \mathscr{F}_{\Delta u}(\sigma),\ \ i = 1, \ldots, n, \tag{2.20}$$

where $\Delta w_{it} = w_{it} - w_{i,t-1}$ represents the first difference for any variable w_{it}, $\Delta y_i = (\Delta y_{i2}, \ldots, \Delta y_{iT})'$, ΔX_i denotes the $(T-1) \times k$ matrix of time-varying covariates with the t-th row $\Delta x_{it}' = (\Delta x_{it1}, \ldots, \Delta x_{itk})$ for $t = 2, \ldots, T$, while $\Delta v_i = (\Delta v_{i2}, \ldots, \Delta v_{iT})'$ and $\Delta u_i = (\Delta u_{i2}, \ldots, \Delta u_{iT})'$ stand for $(T-1) \times 1$ vectors of first-differenced errors. Additionally, $\Psi = \psi^2\Lambda_{T-1}$, where Λ_{T-1}

is a symmetric tridiagonal $(T-1)\times(T-1)$ matrix given by:

$$\Lambda_{T-1} = \begin{pmatrix} 2 & -1 & 0 & \dots & 0 \\ -1 & 2 & -1 & \dots & 0 \\ 0 & -1 & \ddots & \ddots & \vdots \\ \vdots & \ddots & \ddots & \ddots & -1 \\ 0 & 0 & \dots & -1 & 2 \end{pmatrix}. \tag{2.21}$$

Although the normality assumption for v_{it} implies that Δv_i follows a $(T-1)$-variate normal distribution with covariance matrix Ψ, the multivariate distribution of Δu_i is generally unknown. However, the marginal likelihood contribution $L_i^* = \int f(\Delta u_i, \Delta v_i|\theta) d\Delta u_i$ with $\theta = (\beta', \sigma, \psi)'$ can be simulated, given the independence between Δu_i and Δv_i. As illustrated by Belotti and Ilardi (2018), we can express it as:

$$\begin{aligned} L_i^* &= \int f(\Delta u_i, \Delta v_i|\theta) d\Delta u_i = \int f(\Delta v_i|\theta) f(\Delta u_i|\sigma) d\Delta u_i, \\ &= \int f(\Delta y_i|\beta, \psi, \Delta X_i, \Delta u_i) f(\Delta u_i|\sigma) d\Delta u_i. \end{aligned} \tag{2.22}$$

Since $f(\Delta u_i|\sigma, \theta)$ is known and (2.22) lacks a closed-form expression, Belotti and Ilardi (2018) propose two estimation strategies: Marginal Maximum Simulated Likelihood Estimation (MMSLE) and Pairwise Difference Estimation (PDE). MMSLE approximates L_i^* as

$$\begin{aligned} L_i^* &= \mathbb{E}_{\Delta\tilde{u}}\left[\phi_{T-1}(\Delta\varepsilon_i + \sigma\Delta\tilde{u}_i; \Psi)\right] \\ &\approx \bar{L}_i^*(\theta) = \frac{1}{G}\sum_{g=1}^{G} \phi_{T-1}(\Delta\varepsilon_i + \sigma\Delta\tilde{u}_{ig}; \Psi) \end{aligned} \tag{2.23}$$

and solves $\max_\theta \bar{L}_i^*(\theta)$, where $\Delta\varepsilon_i = \Delta y_i - \Delta X_i\beta$, $\phi_{T-1}(\cdot; m, V)$ is the $(T-1)$-variate normal distribution with mean m and covariance matrix V, and G is the number of draws from the multivariate distribution of the first-differenced rescaled inefficiency $\mathscr{F}_{\Delta\tilde{u}}$. MMSLE yields consistent estimates of θ under mild assumptions provided that $n \to \infty$ and $G \to \infty$ with $\sqrt{n}/G \to 0$ (Belotti and Ilardi, 2018, Theorem 1 in Appendix A).

When considering the case of conditional heteroskedastic inefficiency and idiosyncratic error, the simulated likelihood contribution (2.23) takes the form:

$$L_i^* \approx \bar{L}_i^*(\theta) = \frac{1}{G}\sum_{g=1}^{G} \phi_{T-1}(\Delta\varepsilon_i + \Delta\eta_i; \Psi) \tag{2.24}$$

where $\Delta\eta_i = \Delta(\sigma_i \odot \tilde{u}_{ig})$ with $\sigma_i = (\sigma_{i1}, \dots, \sigma_{iT})'$, $\tilde{u}_{ig} = (\tilde{u}_{i1g}, \dots, \tilde{u}_{iTg})'$ represents a draw from

$\mathscr{F}\tilde{u}$. The symbol $\odot$ denotes the standard Hadamard product. This makes the computation of the Marginalized Maximum Score and Log-Likelihood Estimator computationally intensive.

Belotti and Ilardi (2018) propose a Partially Dynamic Estimator (PDE) that not only mitigates the computational burden of MMSLE but also captures the dynamics of inefficiencies. Following the approach outlined by Honoré and Powell (1994), the PDE estimator of Belotti and Ilardi (2018) maximizes $U_n(\theta)$, where

$$U_n(\theta) = n^{-1}\left(\begin{array}{c} T \\ 2 \end{array}\right)^{-1} \sum_{i=1}^{n}\sum_{t=2}^{T}\sum_{s<t} logf\left(\Delta_t^s y_i|\theta, \Delta_t^s x_i\right), \tag{2.25}$$

$\Delta_t^s y_i = y_{it} - y_{is}$ and $\Delta_t^s x_i = x_{it} - x_{is}$. Some observations are of order.

1. $U_n(\theta)$ is a U-statistic, implying that $\hat{\theta} = \arg\max_{\theta} U_n(\theta)$ belongs to the class of U-estimators. Consequently, in addition to achieving consistency under mild assumptions on model variables and parameters, $\hat{\theta}$ is also asymptotically optimal (Belotti and Ilardi, 2018, Theorem 2 in Appendix A). The asymptotic covariance of $\hat{\theta}$ is given by $A_0^{-1}B_0A_0^{-1}$, where

$$\begin{aligned} A_0 &= -\sum_{t=2}^{T}\sum_{s<t}\mathbb{E}\left[\nabla_{\theta\theta} logf\left(\Delta_t^s y_i|\theta_0, \Delta_t^s x_i\right)\right] \\ B_0 &= \mathbb{E}\left\{\left[\sum_{t=2}^{T}\sum_{s<t}\nabla_{\theta} logf\left(\Delta_t^s y_i|\theta_0, \Delta_t^s x_i\right)\right]\left[\sum_{t=2}^{T}\sum_{s<t}\nabla_{\theta} logf\left(\Delta_t^s y_i|\theta_0, \Delta_t^s x_i\right)\right]'\right\}, \end{aligned}$$

   and θ_0 is the unknown parameter vector true value. Note that A_0 and B_0 can be consistently estimated as follows:

$$\begin{aligned} \hat{A}_0 &= \frac{1}{n}\sum_{i=1}^{n}\sum_{t=2}^{T}\sum_{s<t}\nabla_{\theta} logf\left(\Delta_t^s y_i|\hat{\theta}, \Delta_t^s x_i\right)\nabla_{\theta} logf\left(\Delta_t^s y_i|\hat{\theta}, \Delta_t^s x_i\right) \\ \hat{B}_0 &= \hat{A}_0 + \frac{1}{n}\sum_{i=1}^{n}\sum_{t=2}^{T}\sum_{s<t}\sum\sum^{[(k,h)\neq(t,s)]}\nabla_{\theta} logf\left(\Delta_t^s y_i|\hat{\theta}, \Delta_t^s x_i\right)\nabla_{\theta} logf\left(\Delta_t^s y_i|\hat{\theta}, \Delta_t^s x_i\right), \end{aligned}$$

   ∇_θ and $\nabla_{\theta\theta}$ are the first and second derivative of the objective function respectively.

2. Consistency is demonstrated in Belotti and Ilardi (2018, Theorem 1) when $n \to \infty$ and T is fixed. However, consistency also holds if $T \to \infty$ and n is fixed, although this proof requires adapting the large-sample theory for minimizers of U-processes (Honoré and Powell, 1994).

3. A point estimate of the composite error ε_{it} is given by $\hat{\varepsilon}_{it} = y_{it} - \hat{\alpha}_i - x'_{it}\hat{\beta}$, where

$$\hat{\alpha}_i = \frac{1}{T}\sum_{t=1}^{T}(y_{it} - x'_{it}\hat{\beta} + \hat{c}_{it}),\ i = 1, \ldots, n, \tag{2.26}$$

with $\hat{c}_{it} = \mathbb{E}(u_{it}|\hat{\beta}, \hat{\sigma}_{it})$. Note that $\hat{c}_{it} = \hat{\sigma}_{it}$ when $u_{it} \sim \mathscr{E}(\sigma_{it})$ and $\hat{c}_{it} = \sqrt{2\pi^{-1}}\hat{\sigma}_{it}$ when $u_{it} \sim \mathscr{N}^+(0, \sigma^2_{it})$ ($\hat{\sigma}^2_{it} = \hat{\sigma}^2$ under homoskedasticity).

3 Monte Carlo experiment

In this section, we analyze the finite sample properties and performance of the proposed regularized conditional mode estimator outlined in Theorem 2.1, comparing it to both the unregularized conditional mode and conditional mean estimators. We conduct an extensive set of simulations, where we vary: (i) the distribution of inefficiency, (ii) the variance of inefficiency (which may be heteroskedastic), (iii) the time dimension of the panel, and (iv) the cross-sectional dimension of the panel. The data-generating process (DGP) is given by

$$y_{it} = \alpha_i + \beta x_{it} + \nu_{it} - u_{it} \tag{3.1}$$

where $x_{it} = 0.5\alpha_i + 0.5w_{it}$ represents the frontier with $w_{it} \overset{i.i.d.}{\sim} \mathscr{N}(0, 1)$. The unit-specific fixed effects α_i follow independent and identical normal distributions $\mathscr{N}(0, 1)$ across $i = 1, \ldots, n$. The idiosyncratic error component v_{it} follows an independent and identical normal distribution with zero mean and variance ψ^2_{it}. The inefficiency u_{it} follows an independent and identical normal distribution $\mathscr{F}_u(\sigma_{it})$, where $\mathscr{F}_u(\cdot)$ represents a distribution with scale or location-scale parameter σ_{it}. To shorten the presentation, we focus on two sets of distributions for unit inefficiency: (i) $\mathscr{F}_u(\sigma_{it}) \equiv \mathscr{N}^+(0, \sigma^2_{it})$ (half normal with zero mean and time-varying variance σ^2_{it})[3], and (ii) $\mathscr{F}_u(\sigma_{it}) \equiv \mathscr{E}(\sigma_{it})$ (exponential with time-varying scale parameter σ_{it}). The inefficiency variance is modelled to allow for conditional heteroskedasticity, i.e., $\sigma_{it} = exp(\gamma_0 + \gamma_1 z_{it})$, and to simplify, we set $\psi^2_{it} = \psi^2$ for all simulations (homoskedastic idiosyncratic shocks).

The true values of the parameters are: $\beta = 1$, $\psi = 0.25$, and $\gamma_1 = 1$, and $z_{it} \overset{i.i.d.}{\sim} \mathscr{N}(0, 0.0625)$ for all i and t. We vary the parameter γ_0 to allow for variations in the signal-to-noise (STN) ratio. Further discussion of the STN ratio can be found in Belotti et al. (2014). We consider the following values for the signal-to-noise ratio: $\bar{\lambda} = 1, 2, 3, 8$, corresponding to $\gamma_0 = -1.5, -0.8, -0.3, 0.6$, respectively. In all scenarios, we explore the impact of varying cross-sectional dimensions ($n = 100,\ 250$) and panel lengths ($T = 5,\ 10$). Furthermore, we investigate a case with a

[3]Note that the half normal setting corresponds to the truncated normal distribution $u_{it} \sim \mathscr{N}^+(\nu, \sigma^2_{it})$, with mean $\nu = 0$ and time-varying variance σ^2_{it}.

large cross-sectional dimension $n = 1000$ with $T = 5$.

Following Zeebari et al. (2021), the simulations are performed as follows. We simulate n ranked inefficiencies where x_{it} is kept fixed throughout the experiment, and for a given $t = 1, \ldots, T$ and for each of these n samples of inefficiencies, n pseudo-samples of noise terms, v_{it}, are randomly generated from $\mathcal{N}(0, 0.0625)$. This gives $100 \times n$ replications for each unit $i, i = 1, 2, \ldots, n$, and for each of the 40 combinations of parameters (inefficiency distribution, i, t and σ_{it}^2). Secondly, we summarize the simulation results for each firm i at time t using the Mean Square Error (MSE) for three estimators: (i) the Jondrow et al. (1982, JLMS) estimator of the mean of the conditional distribution, $\mathbb{E}(u_{it}|\hat{\varepsilon}_{it})$, developed in Belotti et al. (2014), (ii) the unrestricted estimator of the mode of the conditional distribution of the inefficiency, $\mathbb{M}(u_{it}|\hat{\varepsilon}_{it}, \hat{\theta})$, given in (2.7) and (iii) our regularized estimator of the mode of the conditional distribution of the inefficiency, $\mathbb{M}_r(u_{it}|\hat{\varepsilon}_{it}, \hat{\theta})$, in Theorem 2.1. In a generic form, the MSE of a given estimator $\hat{u}_{it} \in \left\{\mathbb{E}(u_{it}|\hat{\varepsilon}_{it}, \hat{\theta})), \mathbb{M}(u_{it}|\hat{\varepsilon}_{it}, \hat{\theta}), \mathbb{M}_r(u_{it}|\hat{\varepsilon}_{it}, \hat{\theta})\right\}$ for unit i at time t is given by

$$MSE(\hat{u}_{it}) = \frac{1}{10000} \sum_{k=1}^{100} \sum_{j=1}^{100} (\hat{u}_{jit} - u_{kit})^2, \; i = 1, \ldots, n, t = 1, \ldots, T. \tag{3.2}$$

where inner summation is indexed over noise replications j, and the outer summation is indexed over inefficiency replications k. We calculate the Relative RMSE (RelMSE), a measure of relative performance compared to the conditional mean estimator, for both $\mathbb{M}(u_{it}|\hat{\varepsilon}_{it}, \hat{\theta})$ and $\mathbb{M}_r(u_{it}|\hat{\varepsilon}_{it}, \hat{\theta})$ for each $i = 1, \ldots, n$ and each $t = 1, \ldots, T$ as follows:

$$\begin{aligned} RelMSE\big[\mathbb{M}(u_{it}|\hat{\varepsilon}_{it}, \hat{\theta})\big] &= \frac{MSE\big[\mathbb{E}(u_{it}|\hat{\varepsilon}_{it}, \hat{\theta})\big]}{MSE\big[\mathbb{M}(u_{it}|\hat{\varepsilon}_{it}, \hat{\theta})\big]}, \\ RelMSE\big[\mathbb{M}_r(u_{it}|\hat{\varepsilon}_{it}, \hat{\theta})\big] &= \frac{MSE\big[\mathbb{E}(u_{it}|\hat{\varepsilon}_{it}, \hat{\theta})\big]}{MSE\big[\mathbb{M}_r(u_{it}|\hat{\varepsilon}_{it}, \hat{\theta})\big]}. \end{aligned} \tag{3.3}$$

For a given inefficiency estimator, a RelMSE greater than one indicates that the evaluated estimator outperforms the conditional mean estimator. The RelMSE results for the half-normal inefficiency case are illustrated in Figure 3.1, and for the exponential inefficiency case, they are displayed in Figure 3.2. Each figure consists of five panels representing different combinations of (n, T), and each column corresponds to a specific value of the STN ratio. The x-axis in these graphs represents the simulated units ranked by efficiency, with the most efficient unit appearing first and the least efficient unit appearing last. The y-axis displays the mean squared error (MSE) of the estimators relative to the conditional mean estimator.

Upon initial examination of the figures, it becomes apparent that across all simulation settings, the unrestricted conditional mode estimator performs best for the most efficient firms,

while the conditional mean estimator excels for firms with medium-ranking inefficiency. The penalized conditional mode estimator emerges as the top-performing estimator for the most inefficient firms. These findings for the unrestricted conditional mode and conditional mean estimators are consistent with the expectations outlined by Zeebari et al. (2021), who highlighted their shrinkage towards mode and shrinkage towards mean properties.

Figures 3.1 and 3.2 further show that as the STN ratio increases, the restricted mode estimator exhibits a growing advantage over the unrestricted one for firms with higher levels of inefficiency. This is evidenced by the large proportion of inefficient firms where the restricted mode estimator outperforms the unrestricted counterparts. Specifically, as the signal-to-noise (STN) ratio increases, the proportion of inefficient firms favoring the restricted mode estimator grows. Conversely, the percentage of firms–particularly those ranked as least inefficient– where the unrestricted mode estimator outperforms its penalized counterpart decreases, along with the relative mean squared error (MSE).

In Section 4, we employ the proposed methods to assess the cost efficiency of Distribution Network Service Providers (DNSPs), with particular attention to the Australian market.

Figure 3.1: Relative MSE averaged over time dimension for inefficiency distributed as Half Normal distribution

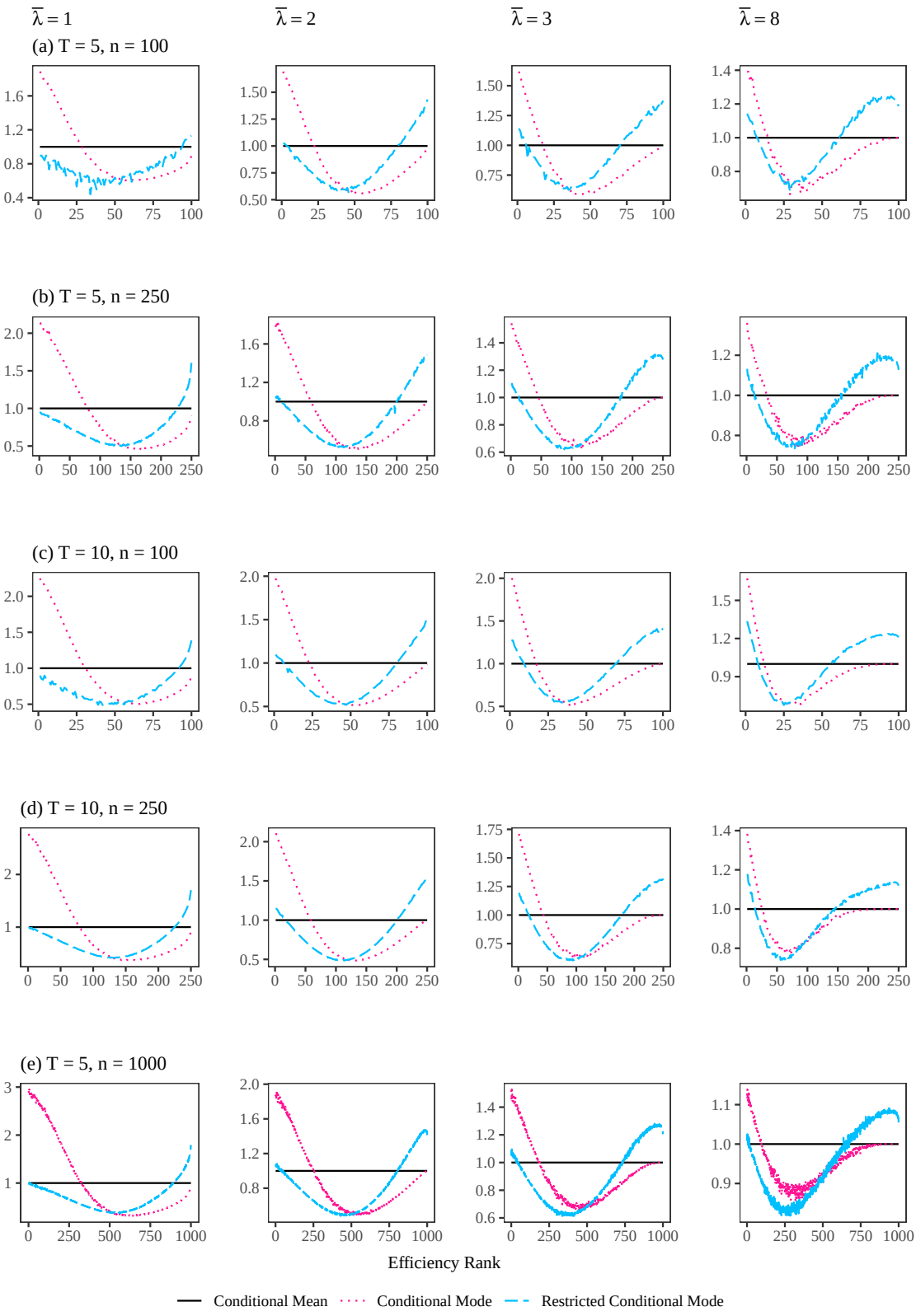

Notes: Total number of replications in each scenario is 10,000. In each sub-plot, simulated firms are ranked from most efficient to most inefficient on the x-axis. The y-axis shows the Relative MSE for each inefficiency estimator. A value above (below) the benchmark line represents better (worse) performance compared to the simulated conditional mean estimator.

Figure 3.2: Relative MSE averaged over time dimension for inefficiency distributed as Exponential distribution

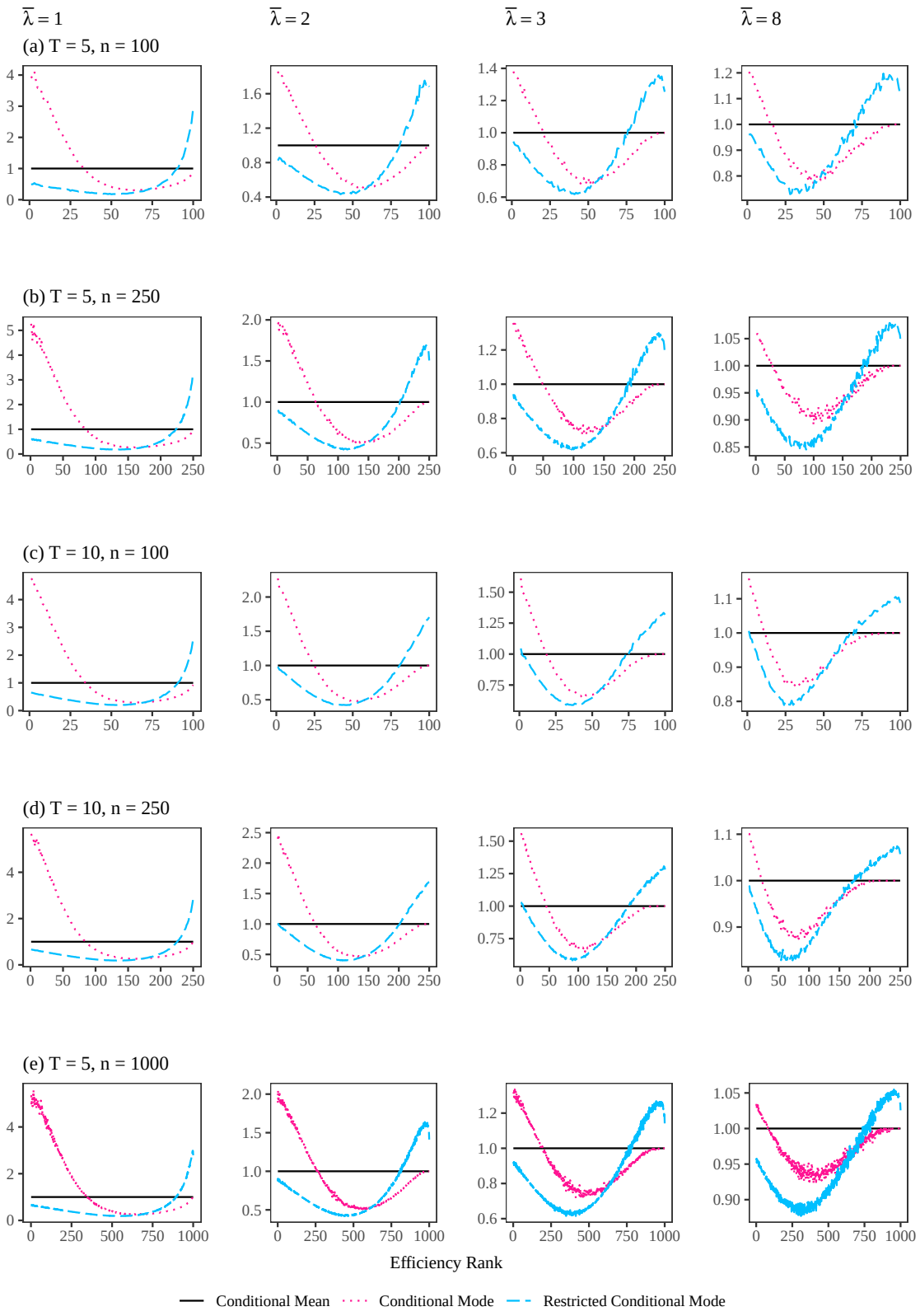

Notes: Total number of replications in each scenario is 10,000. In each sub-plot, simulated firms are ranked from most efficient to most inefficient on the x-axis. The y-axis shows the Relative MSE for each inefficiency estimator. A value above (below) the benchmark line represents better (worse) performance compared to the simulated conditional mean estimator.

4 Empirical applications

This section applies the penalization approach outlined in Section 2 to analyze the cost inefficiency of electricity distribution network service providers (DNSPs) in Australia, Ontario (Canada), and New Zealand.

DNSPs are responsible for the operation of poles, wires, and transformers that facilitate the distribution of electricity to both business and residential customers. Electricity networks are natural monopolies, i.e. a DNSP is the only service provider in the jurisdictions where it operates. Consequently, electricity DNSPs only have weak incentives to minimise their costs. To prevent overinvestments in fixed assets, over-staffed repair and maintenance teams and unproductive administrative procedures, the Australian Energy Regulator (AER), under the National Electricity Law and the National Electricity Rules, uses stochastic frontier models.

These models are used to determine the revenues that an efficient and prudent network business needs at the beginning of each 5-year regulatory period. Then it compares the performance of each DNSP with these benchmarks. Economic benchmarking provides insight into the efficiency of historical network operating expenditures (opex) and capital expenditures (capex), helping the regulator make firm-specific cost predications. In addition, the benchmarks help to understand the factors that influence the magnitude of efficiency, providing insight to both the DNSPs and the regulator on how to improve economic welfare.

In our application, we account for the time-varying characteristics of the inefficiencies, and we also allow for heteroskedasticity, which may explain the variances of inefficiencies and the idiosyncratic error. Section 4.1 provides a detailed overview of the empirical specification that we use.

4.1 Empirical opex cost model

We examine the following translog stochastic frontier panel opex model:

$$\log(\text{opex}_{it}) = \alpha_i + \beta_0 t + \sum_{j=1}^{4} \beta_j \log(\text{X}_{j,it}) + \sum_{j=1}^{4}\sum_{l=1}^{4} \beta_{jl} \log(\text{X}_{j,it}) * \log(\text{X}_{l,it}) + v_{it} + u_{it}, \quad (4.1)$$

where opex_{it} represents the operating expenditure of DNSP i at time t. The vectors $\text{X}_{j,it}$ and $\text{X}_{l,it}$, where $j, l = 1, \ldots, 4$, contain four cost input variables: customer numbers (Customer_Numbers), ratcheted maximum demand (Ratcheted_Max_Demand), circuit length (Circuit_Length), and share of underground cable (Share_Underground_Cable). The parameters β_0, β_j, and β_{jl}, $j, l \in 1, 2, 3, 4$, are unknown, and α_i represents the fixed-effect of DNSP i. The error terms v_{it} and u_{it} denote the idiosyncratic error and the inefficiency of DNSP i, respectively, at time t.

The number of customers is measured as the number of active network connections, reflecting the demand for customer specific services from a DNSP. Circuit length measures the distance over which a DNSP delivers electricity to its customers. It is strongly related to network losses, as well as costs for maintenance and repair. Ratcheted maximum demand (RMD) is the highest demand value observed in any time period up to t, recognizing that capacity must be built to satisfy maximum demand. The share of underground cable reflects the proportion of electricity cables installed underground, which is often seen as a way to enhance the attractiveness of streets or areas, and to reduce the likelihood of outages. However, the widespread implementation of underground power lines presents significant challenges and costs. In Australia, for example, less than 7 per cent of homes are served by underground power, and it is estimated that the cost of undergrounding all existing overhead power lines in the country could reach up to $50 billion. Despite these challenges, efforts to increase the use of underground power vary across regions, with some areas making it compulsory for new suburban subdivisions to have underground power connections.

We assume that the inefficiency term satisfies $u_{it} \overset{i.i.d.}{\sim} \mathscr{F}_u(\sigma_{it})$ (or $u_{it} \overset{i.i.d.}{\sim} \mathscr{F}_u(\nu, \sigma_{it})$ for some constant ν) and the idiosyncratic error term satisfies $v_{it} \overset{i.i.d.}{\sim} N(0, \psi_{it}^2)$, with σ_{it} and ψ_{it} being functions of exogenous covariates. Specifically, we postulate the following relationships:

$$\log(\sigma_{it}) = \gamma_0 + \gamma_1 t + \gamma_2 log(\text{Circuit\_Length}_{it}) + \gamma_3 \log(\text{Share\_Underground\_Cable}_{it}) \quad (4.2)$$

$$\log(\psi_{it}) = \delta_0 + \delta_1 log(\text{Circuit\_Length}_{it}), \quad (4.3)$$

where γ_j $(j = 0, \ldots 3)$ and δ_l $(l = 0, 1)$ capture the effects of circuit length and share of underground cable covariates on the variances of technical inefficiency and idiosyncratic error. Additionally, a time trend is included in both (4.1) and (4.2) to account for persistent changes in the DNSPs' operating expenditures (opex) and the variance of technical inefficiency. Recent research suggests that modeling conditional heteroskedasticity in the variance of technical inefficiency helps mitigate bias in the estimates of the cost frontier and technical inefficiency parameters, and allows for potential non-monotonic efficiency effects (see e.g., Abdul-Salam and Phimister, 2017). The importance of controlling for conditional heteroskedasticity in the variance of technical inefficiency is emphasized by Wang (2002) and Kumbhakar and Lovell (2003), as it aids in understanding the relationship between technical efficiency and its exogenous determinants. Moreover, the conditional heteroskedasticity in the variance of the idiosyncratic error, ψ_{it}^2, can be interpreted as a measure of output (cost) variance (Kumbhakar et al., 2014).

The selection of circuit length and share of underground cable as potential determinants of the variance of technical efficiency stems from their significant impact on the operational

performance and reliability of power distribution systems (see e.g., Jamasb and Söderberg, 2010; Söderberg, 2008). Longer circuit lengths often lead to higher network losses due to increased wire resistance, which results in inefficiencies. The use of underground cables can affect technical efficiency in several ways. Underground cables typically have lower network losses compared to overhead lines because they are insulated and shielded from extreme weather events like storms or falling trees, leading to more reliable and efficient power distribution. The potential for circuit length to determine the variability of the idiosyncratic error likely arises from its influence on the overall complexity and condition of power distribution networks.

4.2 Data and summary statistics

We utilize panel data sourced from the AER, that describes electricity distribution network service providers (DNSPs) in Australia ($N = 13$), New Zealand ($N = 19$), and Ontario, Canada ($N = 31$), spanning the years from 2006 to 2020, i.e., 15 years. The focus of this analysis is on the Australian DNSPs and each of their geographical coverage is displayed in Figure B.1 in Appendix B.

The number of customers served by a DNSP is a critical output metric, as it directly influences demand and the required infrastructure. The higher customer number also increases the customer density, which typically increases network utilization and reduces distribution losses. The length of the circuit, representing the distance over which electricity is delivered, tends to be positively correlated with the opex. That is because circuit length is proportional to network faults (and the need for repair) and network losses. DNSPs install assets to meet maximum demand, indirectly affecting operational expenditure (opex) due to maintenance requirements. Thus, as the MW of maximum demand increases, so does the opex.

Table 4.1 provides summary statistics for key variables in the three countries. To ensure comparability, the opex index for New Zealand and Ontario, originally recorded in New Zealand Dollars and Canadian Dollars respectively, has been converted into Australian Dollars, using 2021 as the base year. The first section of the table presents variables in their original levels, while the second section displays variables transformed into natural logarithms. The opex values are expressed in real terms for each country. Several observations are noteworthy. The opex in Australia is \$268 per customer, and equivalent amounts for NZ and Ontario are \$237 and \$300, respectively. While the three jurisdictions are similar in the sense that they all include substantial rural areas, which drive up cost, they are also culturally, politically and climatologically different. Thus, the three opex per customer values cannot be considered remarkably different.

Regarding the share of underground cable, DNSPs in Australia record an average share of 23.4 percent, while those in NZ and Ontario have shares of 24.5 and 35.9 percent, respectively. Further statistics that describe the Australian DNSPs are available in Tables B.1-B.2 in Appendix B. Variations across states and territories are observed in terms of DNSPs' opex costs. In Victoria, AusNet and Powercor exhibit the highest average opex costs and customer numbers, followed by United Energy and CityPower. Ausgrid dominates in NSW in terms of opex and customer number, while Endeavour has lower opex compared to Essential Energy although it serves approximately 100,000 more customers than Essential Energy. In QLD, both Energex and Ergon Energy exhibit similar average opex, but Energex serves 600,000 more customers. For the remaining states and territories, only SAPower in South Australia averages over 100 million in opex per year, with Evoenergy having the second lowest average opex nationwide, just above CityPower in Victoria.

While the variability in operational expenditure (opex) among Australian DNSPs (std dev = \$137,827) is greater than among those in both Ontario (std dev = \$96,646) and New Zealand (std dev = \$23,663), the disparity in opex costs is comparatively smaller in Australia. This is evident from the coefficients of variation (defined as the ratio between the standard deviation and the mean) of opex, which are 0.70, 2.65, and 1.10 for Australia, Ontario, and New Zealand, respectively. Ontario exhibits the highest disparity, despite all 31 DNSPs being located in the same province.

Table 4.1: Summary Statistics

	Australia			New Zealand			Ontario		
Variable	Obs	Mean	S.D.	Obs	Mean	S.D.	Obs	Mean	S.D.
Operational expenditure (opex) (\$'000)	195	197,291	137,827	285	21,563	23,663	465	36,445	96,646
Price Opex (index)	195	1.023	0.119	285	0.973	0.090	465	0.838	0.074
Ratcheted Max Demand (MW)	195	2,731	1,638	285	304	447	465	625	1,268
Customer Numbers (Numbers)	195	734,152	411,640	285	90,961	126,446	465	121,379	249,960
Circuit Length (kms)	195	55,814	55,921	285	6,499	6,268	465	5,508	21,496
Share of Underground cable	195	0.234	0.150	285	0.245	0.148	465	0.359	0.146
log(Opex/theoex)	195	11.900	0.772	285	9.646	0.760	465	9.690	1.037
log(Customer Numbers)	195	1.912	0.630	285	-0.526	0.893	465	-0.479	0.983
log(Circuit Length)	195	2.112	1.222	285	0.299	0.647	465	-1.069	1.151
log(Ratcheted Max Demand)	195	1.800	0.636	285	-0.784	0.952	465	-0.274	1.004
log(Share of Underground cable)	195	-1.736	0.836	285	-1.604	0.672	465	-1.141	0.548

4.3 Estimation and results

We estimate model (4.1)-(4.3) under three parametric distributional assumptions for the technical inefficiency term: (i) $u_{it} \sim \mathscr{N}^{+}(\nu, \sigma_{it}^2)$ (truncated normal with unknown constant mean ν and time-varying variance σ_{it}^2), (ii) $u_{it} \sim \mathscr{E}(\sigma_{it})$ (exponential with time-varying trending scale

parameter σ_{it}), and (ii) $u_{it} \sim \mathscr{N}^{+}(0, \sigma_{it}^2)$ (half normal with zero mean and time-varying variance σ_{it}^2). To shorten the presentation, we only discuss the results related to the truncated normal time-varying inefficiency variance, which are reported in Table 4.2. Those with time-varying exponential and half normal inefficiencies are similar to those presented here and are shown in Tables B.3-B.4 in the appendix. The left-hand side of Table 4.2 shows the estimates of the cost frontier, i.e., equation (4.1), while the right-hand side contains the estimates of the variance specification, including both the technical inefficiency and the idiosyncratic error, i.e., equations (4.2)-(4.3).

Beginning with our examination of the cost function estimates, we observe that the presence of underground cable had an insignificant impact and is highly correlated with ratcheted maximum demand. Consequently, we omitted it from the cost function but retained its inclusion in the variance equations. Circuit length and its interactions with other covariates are statistically significance at least at the 10 percent level. Customer number has a large positive effect on opex. Moreover, opex is negatively related to ratcheted maximum demand, although the latter effect is not statistically significant even at the 10 percent level. The interaction between customer number and ratcheted maximum demand is negative and significant at the 1 percent level, meaning that their degree of substitutability is strong. Also, both covariates are strongly correlated and strongly complementary with circuit length. The coefficients on the interaction terms capture the impact of one input on the marginal effect of another. Therefore, once they are accounted for, the marginal effects of all covariates depend on the other covariates. There is a strong positive linear trend component in the opex cost function, with an estimated coefficient of 0.012 that is significant at the 1 percent level.

Next, looking at the impact of exogenous factors on technical efficiency in the right-hand side of the table, a negative coefficient implies that a higher variable value leads to higher efficiency and/or lower cost variance. Circuit length is positively related to inefficiency while the impact of the share of underground cable is U-shaped. This suggests that DNSPs with higher share of underground cable are more efficient. Circuit length also has a U-shape impact on the cost variance, indicating a complex relationship between network size and opex.

These results align with previous studies that have pointed out the importance of accounting for conditional heteroskedasticity in the variances of technical inefficiency and in the idiosyncratic error, see e.g., Abdul-Salam and Phimister (2017), Wang (2002), Kumbhakar and Lovell (2003), and Kumbhakar et al. (2014). Results are qualitatively similar when the inefficiencies are generated by exponential and truncated normal distributions, as displayed in Tables B.3 and B.4 in Appendix B.

Table 4.2: Cost frontier and technical efficiency estimates - Truncated Normal Distribution

Cost Frontier Estimates		**Variance estimates technical inefficiency & idiosyncratic shock**	
Variable	Coefficient	Variable	Coefficient
log (Customer Number)	0.439***	*Heteroscedasticity in technical inefficiency variance*	
	[0.1501]		
log (Ratcheted Max Demand)	0.122	Constant	-1.134***
	[0.1237]		[0.3643]
log (Circuit Length)	0.209*	log (Circuit Length)	0.291***
	[0.1074]		[0.0942]
log (Circuit Length) * log (Customer Number)	0.108*	log (Share of Underground Cable)	-0.121
	[0.0614]		[0.2872]
log (Customer Number) * log (Ratcheted Max Demand)	-0.457***	log (Share of Underground Cable)^2	0.007
	[0.0903]		[0.0999]
log (Circuit Length) * log (Ratcheted Max Demand)	0.262**	log (Share of Underground Cable) * log (Circuit Length)	0.165***
	[0.1063]		[0.0570]
Year trend	0.012***	Year trend	-0.006
	[0.0018]		[0.0066]
		Heteroscedasticity in idiosyncratic error variance	
		Constant	-4.035***
			[0.5211]
		log (Circuit Length)	-0.013
			[0.1001]
		log (Circuit Length)^2	0.132**
			[0.0518]
		Truncated Distribution Mean	
		Constant	-0.898
			[0.8417]
Observations	945		

Note: The left-hand side shows the estimates of the cost frontier, i.e., equation (4.1), and the right-hand side contains the estimates of the variance specification for both the technical inefficiency and the idiosyncratic error, i.e., equations (4.2)-(4.3), as well as the truncated distribution mean. Standard errors are in parentheses. ***, **, and * indicate statistical significance at 1%, 5% and 10% nominal level, respectively.

Figure 4.1 presents a graph of the estimated relative technical efficiencies (RTE) based on the truncated normal inefficiency distribution for Australian Distribution Network Service Providers (DNSP) for the period 2006 to 2020. Relative efficiency is benchmarked against the JLMS conditional mean, which explains why the graphs for the conditional mean estimates consistently show a value of one across all time periods and for all DNSPs.

For most DNSPs, our restricted conditional mode estimator produces lower technical inefficiency estimates compared to the standard unrestricted mode estimator. This trend is particularly evident among DNSPs further from the efficiency frontier, such as Endeavour Energy, South Australia Power, and Energex (refer to Table 4.4 for DNSP rankings), where the conditional mean and unrestricted mode estimators tend to overestimate efficiency.

The conditional mode estimator consistently yields relative technical efficiency (RTE) estimates closer to the JLMS conditional mean. In contrast, the RTE estimates from the restricted conditional mode exhibit greater variability over time. This variability reflects the impact of penalization on efficiency estimates and is more pronounced among DNSPs closer to the efficiency frontier, such as Essential Energy, Ergon Energy, and Powercor, compared to those further from the frontier.

For most DNSPs, the restricted mode indicates an overall pattern of improving efficiency over time relative to the JLMS conditional mean and the unrestricted conditional mode estimators. This suggests that the restricted conditional mode may be better suited to identifying changes in relative performance over time.

The following conclusions emerge from this empirical analysis:

1. **Technical Efficiency Varies Over Time**. The analysis demonstrates that technical efficiency changes over time, particularly when using the more accurate restricted mode approach. A modeling framework that cannot accurately capture time-varying inefficiency faces two significant challenges: either adding a large buffer to its demands, reducing overall efficiency, or risking the imposition of unreasonable demands on DNSPs, which could lead to adverse outcomes.

2. **Comparison with AER Rankings**. To assess the differences between our results and those produced by the Australian Energy Regulator (AER), we calculate the mean efficiency rank for each DNSP based on Table 4.3. The AER's rankings for the 2006–2020 period, derived using the JLMS estimator, are listed in the right-most column of Table 4.4, as reported in AER's 2021 annual report (AER, 2021). A comparison reveals notable discrepancies between our penalization-based approach and the simpler cross-sectional model used by the AER. For instance, the AER ranks Evoenergy as the second-lowest

Figure 4.1: Relative technical efficiency for each Australian DNSPs assuming Truncated Normal distribution for inefficiencies

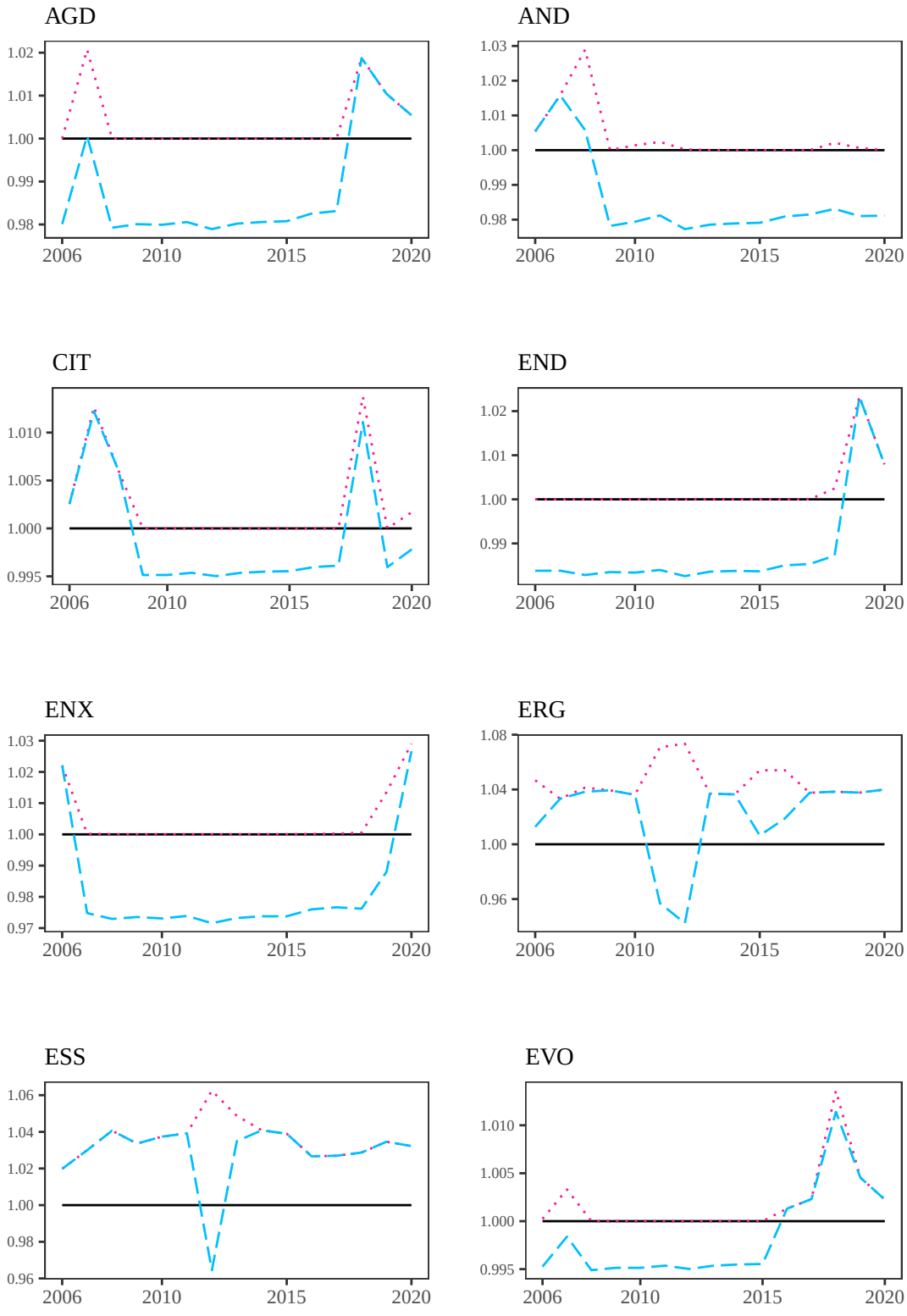

(Continued on next page)

Relative technical efficiency for each Australian DNSPs assuming Truncated Normal distribution for inefficiencies (continued from previous page)

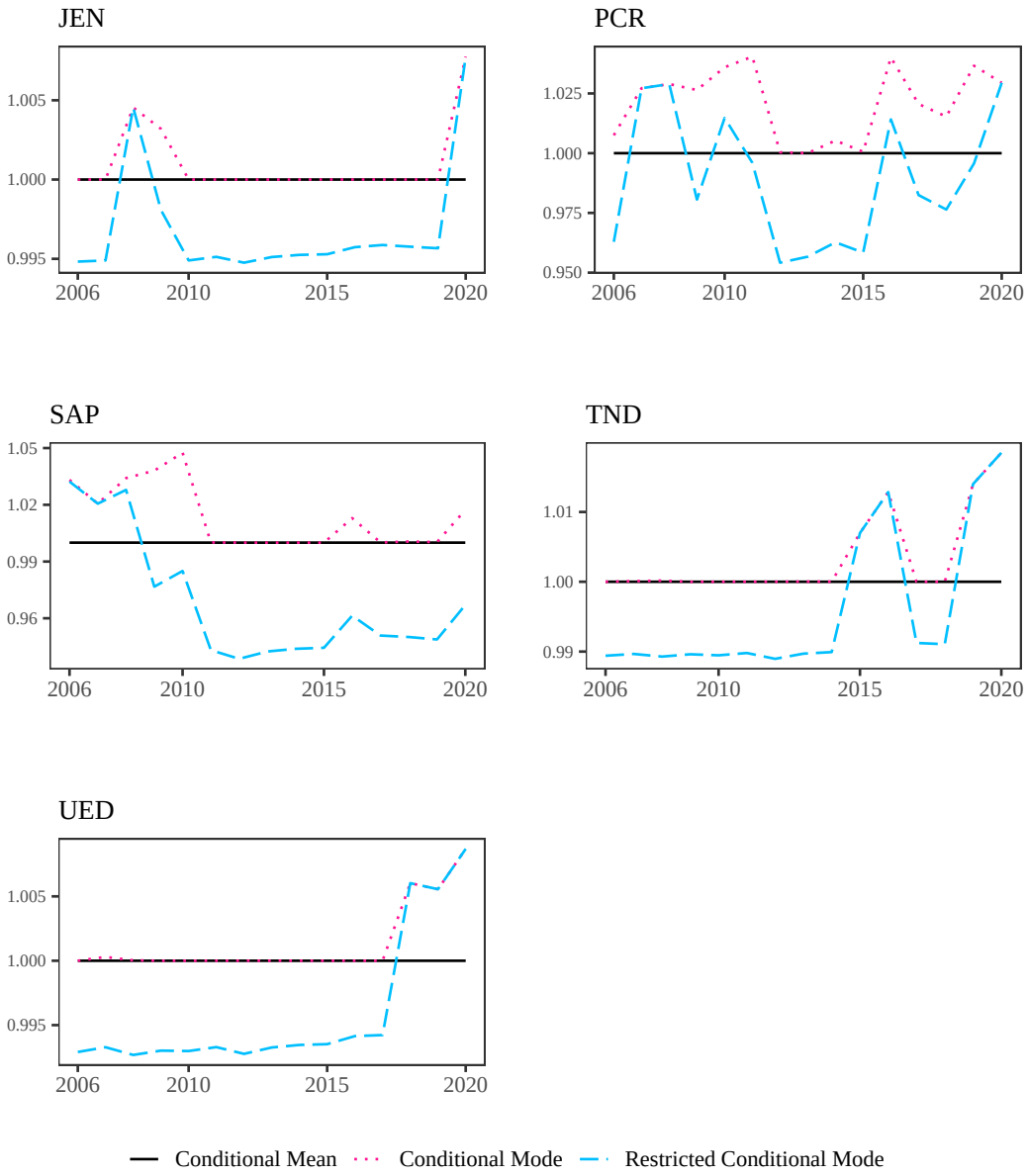

performer (12th place), while our analysis assigns it an average rank of 6.33, making it the fourth best. Similarly, the AER ranks South Australia Power as the third best, whereas our approach places it at an average rank of 8.87.

These discrepancies highlight the risks of relying on less sophisticated models. Misleading rankings can lead government agencies to make decisions that may harm economic outcomes, underscoring the need for robust, time-sensitive modeling approaches in regulatory decision-making.

5 Conclusion

In this paper, we develop a penalization approach for estimating inefficiency in stochastic frontier panel models. The value of such an estimator is that it solves two problems that have not previously been solved simultaneously.

The first problem is that the standard JLMS estimator estimates the mean (and mode) of inefficiency conditioned on the composite error. This leads to a distribution of inefficiencies that is different from the true distribution. Moreover, the conditional estimator relies on an estimated composite error rather than the actual composite error. This leads to inaccuracies in estimating inefficiencies. Zeebari et al. (2023) addressed these issues for cross-sectional data.

The second problem is that SFA panel models do not regularly incorporate conditional heteroskedasticity, time variation in the inefficiency and idiosyncratic shock distributions. This has recently been dealt with by Belotti and Ilardi (2018).

We address both of these problems in this paper. We take Belotti and Ilardi's model as a starting point and add a penalization approach – similar to Zeebari et al. (2023), but to a panel data setting. Monte Carlo simulations show that our proposed approach generally out-perform the JLMS and unpenalized estimators. An application based on data from the Australian Energy Regulator (AER) show that our results are markedly different from those produced by AER. Consequently, we recommend AER, and other regulatory agencies, to use penalization estimators and to incorporate conditional heteroskedasticity and time variation in the inefficiency, as well as in the idiosyncratic shock distributions.

Table 4.3: Efficiency Rank of DNSPs for Truncated Normal Inefficiency

Rank	2006	2007	2008	2009	2010	2011	2012	2013	2014	2015	2016	2017	2018	2019	2020
1	CIT	ERG	CIT	ERG	ERG	ESS	ESS	ERG	ERG	ESS	EVO	EVO	AGD	EVO	EVO
2	ENX	ESS	ESS	ESS	ESS	PCR	ERG	ESS	ESS	TND	ESS	ERG	ERG	AGD	AGD
3	ESS	PCR	JEN	JEN	PCR	CIT	AND	TND	TND	ERG	TND	ESS	ESS	ERG	END
4	AND	SAP	PCR	ACT	SAP	AND	PCR	END	PCR	UED	PCR	PCR	UED	ESS	ERG
5	SAP	AND	ERG	PCR	AND	ERG	JEN	AGD	JEN	JEN	ERG	AGD	ACT	TND	ESS
6	ERG	CIT	SAP	SAP	UED	JEN	END	JEN	UED	CIT	SAP	CIT	CIT	UED	JEN
7	EVO	EVO	AND	CIT	EVO	EVO	SAP	UED	AND	PCR	ENX	ENX	END	END	PCR
8	JEN	AGD	EVO	UED	JEN	TND	CIT	AND	END	END	CIT	UED	PCR	PCR	TND
9	UED	UED	UED	AND	CIT	END	EVO	CIT	CIT	AND	JEN	END	AND	ENX	UED
10	TND	TND	TND	TND	END	SAP	TND	PCR	AGD	ENX	AGD	AND	JEN	CIT	ENX
11	PCR	ENX	ENX	ENX	ENX	ENX	UED	SAP	ENX	SAP	UED	JEN	TND	AND	CIT
12	END	JEN	END	AGD	TND	AGD	ENX	EVO	SAP	ACT	END	TND	ENX	JEN	SAP
13	AGD	END	AGD	END	AGD	UED	AGD	ENX	EVO	AGD	AND	SAP	SAP	SAP	AND

Table 4.4: Ranking of DNSP by efficiency– Truncated normal distribution

DNSP	Minimum†	Maximum†	Median †	Mean †	AER's rank‡
ESS	1	5	2	2.33	7
ERG	1	6	2	2.8	11
PCR	2	11	4	5.6	1
EVO	1	13	7	6.33	12
CIT	1	11	7	6.67	2
JEN	3	12	6	7.27	8
AND	3	13	8	7.8	6
TND	2	12	10	7.8	4
UED	4	13	8	8.0	5
AGD	1	13	10	8.8	13
END	3	13	9	8.87	10
SAP	4	13	10	8.87	3
ENX	2	13	11	9.87	9

Notes. † Results generated by penalization approach described in Section 2.2 in this paper.
‡ Results generated by the JLMS estimator, i.e., cross-sectional SFA model with pooled data.

Acknowledgements

Doko Tchatoka and Söderberg acknowledge financial support from the Ratio Institute through the Research Fellowship UA216029 at the University of Adelaide. They also extend their gratitude to Research Fellow Julia Puellbeck for her invaluable support during the project's initial stages. Additionally, Doko Tchatoka acknowledges funding from the Australian Research Council through the Discovery Grants DP210103094. This paper forms part of the research activities undertaken at the School of Economics and Public Policy at The University of Adelaide.

Appendices

A Proofs

Proof of Theorem 2.1. First, note that the first-order condition (F.O.C) of maximization problem can be written as:

$$\begin{cases} \frac{\partial}{\partial u_{it}}\left[\mathscr{L}(u_{1t},\ldots,u_{nt},\lambda_t;\theta)\right]\mid_{(u_{it},\lambda_t)=(\tilde{u}_{it},\tilde{\lambda}_t)}= \frac{\phi'(\varepsilon_{it}+\tilde{u}_{it};0,\psi_{it}^2)}{\phi(\varepsilon_{it}+\tilde{u}_{it};0,\psi_{it}^2)}+\frac{f_u'(\tilde{u}_{it})}{f_u(\tilde{u}_{it})}+\tilde{\lambda}_t=0,\ i=1,\ldots,n \\ \frac{\partial}{\partial \lambda_t}\left[\mathscr{L}(u_{1t},\ldots,u_{nt},\lambda_t;\theta)\right]\mid_{(u_{it},\lambda_t)=(\tilde{u}_{it},\tilde{\lambda}_t)}= \sum_{i=1}^n(\varepsilon_{it}+\tilde{u}_{it})=0, \end{cases} \tag{A.1}$$

where $\phi'(\varepsilon_{it}+u_{it};0,\psi_{it}^2)=\partial\phi(\varepsilon_{it}+u_{it};0,\psi_{it}^2)/\partial u_{it}$ and $f_u'(u_{it})=\partial f_u(u_{it})/\partial u_{it}$. Since $v_{it}\sim\mathscr{N}(0,\psi_{it}^2)$, we have $\phi'(\varepsilon_{it}+u_{it};0,\psi_{it}^2)=-\left(\frac{\varepsilon_{it}+u_{it}}{\psi_{it}^2}\right)\phi(\varepsilon_{it}+u_{it};0,\psi_{it}^2)$ for all i and t.

(a) If $u_{it}\sim\mathscr{N}^+(0,\sigma_{it}^2)$, then $f_u'(u_{it})=-\left(\frac{u_{it}}{\sigma_{it}^2}\right)f_u(u_{it})$ and we can write (A.1) as:

$$-\frac{\varepsilon_{it}+\tilde{u}_{it}}{\psi_{it}^2}-\frac{\tilde{u}_{it}}{\sigma_{it}^2}+\tilde{\lambda}_t = 0 \iff \tilde{u}_{it}=\frac{\sigma_{it}^2\psi_{it}^2\tilde{\lambda}_t}{\sigma_{it}^2+\psi_{it}^2}-\frac{\sigma_{it}^2\varepsilon_{it}}{\sigma_{it}^2+\psi_{it}^2},\ i=1,\ldots,n \tag{A.2}$$

$$\sum_{i=1}^n(\varepsilon_{it}+\tilde{u}_{it}) = 0. \tag{A.3}$$

We can also write the first equation of the equivalence in (A.2) as $-(\varepsilon_{it}+\tilde{u}_{it})=-\psi_{it}^2\tilde{\lambda}_t+\frac{\psi_{it}^2\tilde{u}_{it}}{\sigma_{it}^2}$, and by averaging this over i and using (A.3), we get $\bar{\psi}_t^2\tilde{\lambda}_t=\bar{\tilde{u}}_t^*$, where $\bar{\psi}_t^2=\frac{1}{n}\sum_{i=1}^n\psi_{it}^2$ and $\bar{\tilde{u}}_t^*=\frac{1}{n}\sum_{i=1}^n\left(\frac{\psi_{it}^2}{\sigma_{it}^2}\right)\tilde{u}_{it}$. But, it is clear from the second equation of the equivalence in (A.2) that $\bar{\tilde{u}}_t^*=\tilde{\lambda}_t\frac{1}{n}\sum_{i=1}^n\left(\frac{\psi_{it}^4}{\sigma_{it}^2+\psi_{it}^2}\right)-\frac{1}{n}\sum_{i=1}^n\left(\frac{\psi_{it}^2}{\sigma_{it}^2+\psi_{it}^2}\right)\varepsilon_{it}=\bar{\psi}_t^{-2}\bar{\eta}_t\bar{\tilde{u}}_t^*-\bar{\varepsilon}_t^*$, where $\bar{\eta}_t=\frac{1}{n}\sum_{i=1}^n\left(\frac{\psi_{it}^4}{\sigma_{it}^2+\psi_{it}^2}\right)$ and $\bar{\varepsilon}_t^*=\frac{1}{n}\sum_{i=1}^n\left(\frac{\psi_{it}^2}{\sigma_{it}^2+\psi_{it}^2}\right)\varepsilon_{it}$. As such, we have $\bar{\tilde{u}}_t^*=-(1-\bar{\psi}_t^{-2}\bar{\eta}_t)^{-1}\bar{\varepsilon}_t^*$, so that $\tilde{\lambda}_t=\bar{\psi}_t^{-2}\bar{\tilde{u}}_t^*=-\bar{\psi}_t^{-2}(1-\bar{\psi}_t^{-2}\bar{\eta}_t)^{-1}\bar{\varepsilon}_t^*=-(\bar{\psi}_t^2-\bar{\eta}_t)^{-1}\bar{\varepsilon}_t^*$. Therefore, we

get

$$\tilde{u}_{it}(\varepsilon_{it},\theta) \equiv \tilde{u}_{it} = -\Big(\frac{\sigma_{it}^2}{\sigma_{it}^2+\psi_{it}^2}\Big)\varepsilon_{it} - \Big(\frac{\sigma_{it}^2\psi_{it}^2}{(\sigma_{it}^2+\psi_{it}^2)(\bar{\psi}_t^2-\bar{\eta}_t)}\Big)\bar{\varepsilon}_t^*,\ i=1,\ldots,n. \quad (A.4)$$

(*b*) $u_{it} \sim \mathscr{E}(\sigma_{it})$, then $f_u'(u_{it}) = -\big(\frac{1}{\sigma_{it}}\big) f_u(u_{it})$ and we can write (A.1) as:

$$-\frac{\varepsilon_{it}+\tilde{u}_{it}}{\psi_{it}^2} - \frac{1}{\sigma_{it}} + \tilde{\lambda}_t = 0 \iff \tilde{u}_{it} = -\varepsilon_{it} + \psi_{it}^2\tilde{\lambda}_t - \frac{\psi_{it}^2}{\sigma_{it}},\ i=1,\ldots,n \quad (A.5)$$

$$\sum_{i=1}^{n}(\varepsilon_{it}+\tilde{u}_{it}) = 0. \quad (A.6)$$

By proceeding as in the above proof of (a), we get

$$\tilde{u}_{it}(\varepsilon_{it},\theta) \equiv \tilde{u}_{it} = -\varepsilon_{it} + \Big(\frac{\psi_{it}^2}{\bar{\psi}_t^2}\Big)\bar{\zeta}_t - \frac{\psi_{it}^2}{\sigma_{it}},\ i=1,\ldots,n, \quad (A.7)$$

where $\bar{\zeta}_t = \frac{1}{n}\sum_{i=1}^{n}\big(\frac{\psi_{it}^2}{\sigma_{it}}\big)$.

(*c*) If $u_{it} \sim \mathscr{N}^+(\nu,\sigma_{it}^2)$, then $f_u'(u_{it}) = -\big(\frac{(u_{it}-\nu)}{\sigma_{it}^2}\big) f_u(u_{it})$ and we can write (A.1) as:

$$-\frac{\varepsilon_{it}+\tilde{u}_{it}}{\psi_{it}^2} - \frac{\tilde{u}_{it}-\nu}{\sigma_{it}^2} + \tilde{\lambda}_t = 0 \iff \tilde{u}_{it} = \frac{\sigma_{it}^2\psi_{it}^2\tilde{\lambda}_t}{\sigma_{it}^2+\psi_{it}^2} - \frac{\sigma_{it}^2\varepsilon_{it}}{\sigma_{it}^2+\psi_{it}^2} + \frac{\psi_{it}^2\nu}{\sigma_{it}^2+\psi_{it}^2} \quad (A.8)$$

$$\sum_{i=1}^{n}(\varepsilon_{it}+\tilde{u}_{it}) = 0. \quad (A.9)$$

We can also write the first equation of the equivalence in (A.2) as $-(\varepsilon_{it}+\tilde{u}_{it}) = -\psi_{it}^2\tilde{\lambda}_t + \frac{\psi_{it}^2\tilde{u}_{it}}{\sigma_{it}^2} - \frac{\psi_{it}^2\nu}{\sigma_{it}^2}$, and by averaging this over i and using (A.9), we have $\bar{\psi}_t^2\tilde{\lambda}_t = \bar{\tilde{u}}_t^* - \bar{\omega}_t^2\nu$, $\bar{\psi}_t^2$ and $\bar{\tilde{u}}_t^*$ are defined in the above proof of (a), and $\bar{\omega}_t^2 = \frac{1}{n}\sum_{i=1}^{n}\big(\frac{\psi_{it}^2}{\sigma_{it}^2}\big)$. But, from the second equation of the equivalence in (A.8), we also have $\bar{\tilde{u}}_t^* = \tilde{\lambda}_t\bar{\eta}_t - \bar{\varepsilon}_t^* + \nu\bar{\kappa}_t = \bar{\psi}_t^{-2}\bar{\eta}_t\bar{\tilde{u}}_t^* - \bar{\psi}_t^{-2}\bar{\omega}_t^2\bar{\eta}_t\nu - \bar{\varepsilon}_t^* + \nu\bar{\kappa}_t$, where $\bar{\kappa}_t = \frac{1}{n}\sum_{i=1}^{n}\big(\frac{\psi_{it}^4}{\sigma_{it}^2(\sigma_{it}^2+\psi_{it}^2)}\big)$, all $\bar{\eta}_t$, $\bar{\varepsilon}_t^*$ and $\bar{\tilde{u}}_t^*$ are defined as in (a). This implies that $\bar{\tilde{u}}_t^* = -(1-\bar{\psi}_t^{-2}\bar{\eta}_t)^{-1}\bar{\varepsilon}_t^* - (1-\bar{\psi}_t^{-2}\bar{\eta}_t)^{-1}\bar{\psi}_t^{-2}\bar{\omega}_t^2\bar{\eta}_t\nu + (1-\bar{\psi}_t^{-2}\bar{\eta}_t)^{-1}\nu\bar{\kappa}_t = -(1-\bar{\psi}_t^{-2}\bar{\eta}_t)^{-1}\bar{\varepsilon}_t^* - (\bar{\psi}_t^2-\bar{\eta}_t)^{-1}\bar{\omega}_t^2\bar{\eta}_t\nu + (1-\bar{\psi}_t^{-2}\bar{\eta}_t)^{-1}\nu\bar{\kappa}_t$. Thus, $\tilde{\lambda}_t = \bar{\psi}_t^{-2}\bar{\tilde{u}}_t^* - \bar{\omega}_t^2\nu\bar{\psi}_t^{-2} = -(\bar{\psi}_t^2-\bar{\eta}_t)^{-1}\bar{\varepsilon}_t^* - \bar{\psi}_t^{-2}(\bar{\psi}_t^2-\bar{\eta}_t)^{-1}\bar{\omega}_t^2\bar{\eta}_t\nu + (\bar{\psi}_t^2-\bar{\eta}_t)^{-1}\nu\bar{\kappa}_t - \bar{\omega}_t^2\nu\bar{\psi}_t^{-2}$. Therefore, we get

$$\begin{aligned}\tilde{u}_{it}(\varepsilon_{it},\theta) = {} & -\Big(\frac{\sigma_{it}^2}{\sigma_{it}^2+\psi_{it}^2}\Big)\varepsilon_{it} - \Big(\frac{\sigma_{it}^2\psi_{it}^2}{(\sigma_{it}^2+\psi_{it}^2)(\bar{\psi}_t^2-\bar{\eta}_t)}\Big)\bar{\varepsilon}_t^* + \\ & -\frac{\sigma_{it}^2\psi_{it}^2}{(\sigma_{it}^2+\psi_{it}^2)(\bar{\psi}_t^2-\bar{\eta}_t)}\left[\frac{\bar{\omega}_t^2\bar{\eta}_t}{\bar{\psi}_t^2} + \frac{(\bar{\psi}_t^2-\bar{\eta}_t)\bar{\omega}_t^2}{\bar{\psi}_t^2} - \frac{(\bar{\psi}_t^2-\bar{\eta}_t)}{\sigma_{it}^2} - \bar{\kappa}_t\right]\nu \\ & \text{for all } i=1,\ldots,n. \end{aligned} \quad (A.10)$$

□

B Additional Descriptive Statistics

B.1 Tables and Figures– Descriptive statistics

Figure B.1: Electricity distribution network service providers in Australia

Note. The map shows the geographic distribution of the DNSPs Asutralia wide and in each state and territory. Australian Capital Territory– ACT (ActewAGL, Evoenergy since 2018); New South Wales– AGD (Ausgrid), END (Endeavour Energy), ESS (Essential Energy); Queensland– ENX (Energex), ERG (Ergon Energy); South Australia– SAP (SA Power Networks); Tasmania– TND (TasNetworks Distribution); Victoria– AND (AusNet Service Distribution), CIT (CitiPower), JEN (Jemena Electricity Networks), PCR (Powercor), UED (United Energy Distribution).

Table B.1: Detailed summary Statistics: VIC, NSW and QLD

Victoria

	AND		CIT		JEN		PCR		UED	
Variable	Mean	S. D.	Mean	S. D.	Mean	S. D.	Mean	S. D.	Mean	S. D.
Operational expenditure (opex) ($'000)	167,475	44,496	46,216	10,396	66,037	13,798	155,405	30,159	109,863	18,553
Price Opex (index)	1.032	0.121	1.032	0.121	1.032	0.121	1.032	0.121	1.032	0.121
Ratcheted Max Demand (MW)	1,911	123	1,449	61	998	57	2,490	169	2,078	135
Customer Numbers (Numbers)	683,907	53,815	322,233	17,202	324,995	23,722	758,958	64,549	654,528	28,454
Circuit Length (kms)	43,762	1,338	4,327	226	6,170	305	73,916	1,413	12,876	353
Share of Underground cable	0.127	0.023	0.480	0.024	0.276	0.033	0.071	0.016	0.215	0.025
log(Opex/theoex)	11.965	0.188	10.689	0.152	11.051	0.119	11.910	0.106	11.568	0.110
log(Customer Numbers)	2.015	0.078	1.264	0.054	1.271	0.072	2.118	0.085	1.973	0.043
log(Circuit Length)	2.471	0.031	0.156	0.053	0.511	0.049	2.995	0.019	1.247	0.027
log(Ratcheted Max Demand)	1.629	0.067	1.354	0.043	0.980	0.060	1.894	0.072	1.713	0.069
log(Share of Underground cable)	-2.077	0.180	-0.736	0.052	-1.294	0.121	-2.669	0.235	-1.544	0.113

New South Wales & Queensland

	AGD		END		ESS		ENX		ERG	
Variable	Mean	S. D.	Mean	S. D.	Mean	S. D.	Mean	S. D.	Mean	S. D.
Operational expenditure (opex) ($'000)	484,451	87,550	233,987	36,661	340,047	63,506	317,949	60,115	321,371	49,279
Price Opex (index)	1.018	0.124	1.018	0.124	1.018	0.124	1.018	0.124	1.018	0.124
Ratcheted Max Demand (MW)	6,453	165	4,113	205	2,766	215	5,132	330	3,162	147
Customer Numbers (Numbers)	1,645,478	68,936	932,839	63,323	854,904	41,009	1,364,455	94,398	703,537	45,871
Circuit Length (kms)	40,650	1,188	35,283	1,996	191,189	3,013	51,472	2,615	151,729	1,361
Share of Underground cable	0.360	0.020	0.337	0.041	0.039	0.007	0.320	0.031	0.050	0.011
log(Opex/theoex)	13.064	0.171	12.340	0.100	12.707	0.140	12.640	0.120	12.658	0.076
log(Customer Numbers)	2.895	0.042	2.326	0.067	2.240	0.048	2.706	0.069	2.044	0.066
log(Circuit Length)	2.397	0.029	2.254	0.056	3.945	0.016	2.632	0.051	3.714	0.009
log(Ratcheted Max Demand)	2.848	0.026	2.397	0.051	1.998	0.078	2.617	0.068	2.134	0.048
log(Share of Underground cable)	-1.022	0.055	-1.095	0.120	-3.261	0.186	-1.144	0.100	-3.035	0.268

Table B.2: Detailed summary Statistics - ACT, SA and TAS

	ACT		SAP		TND	
Variable	Mean	S. D.	Mean	S. D.	Mean	S. D.
Operational expenditure (opex) ($'000)	51,412	13,677	199,319	52,615	71,254	13,393
Price Opex (index)	1.018	0.124	1.018	0.124	1.018	0.124
Ratcheted Max Demand (MW)	682	45	3,120	156	1,148	23
Customer Numbers (Numbers)	177,309	17,057	844,442	43,549	276,390	13,184
Circuit Length (kms)	4,423	221	87,642	1,473	22,146	665
Share of Underground cable	0.476	0.031	0.188	0.013	0.103	0.010
log(Opex/theoex)	10.804	0.209	12.154	0.183	11.145	0.121
log(Customer Numbers)	0.663	0.095	2.227	0.052	1.110	0.048
log(Circuit Length)	0.178	0.050	3.165	0.017	1.789	0.030
log(Ratcheted Max Demand)	0.599	0.066	2.120	0.052	1.121	0.021
log(Share of Underground cable)	-0.744	0.066	-1.675	0.071	-2.273	0.095

B.2 Tables and Figures– Estimation

Table B.3: Cost frontier and technical efficiency estimates - Exponential Distribution

Cost Frontier Estimates		**Variance estimates technical inefficiency & idiosyncratic shock**	
Variable	Coefficient	Variable	Coefficient
log (Customer Number)	0.458***	*Heteroscedasticity in technical inefficiency variance*	
	[0.1509]		
log (Ratcheted Max Demand)	0.119	Constant	-2.489***
	[0.1225]		[0.3919]
log (Circuit Length)	0.201*	log (Circuit Length)	0.513***
	[0.1077]		[0.1873]
log (Circuit Length) * log (Customer Number)	0.099	log (Share of Underground Cable)	-0.253
	[0.0640]		[0.5494]
log (Customer Number) * log (Ratcheted Max Demand)	-0.446***	log (Share of Underground Cable)^2	0
	[0.0878]		[0.1889]
log (Circuit Length) * log (Ratcheted Max Demand)	0.263**	log (Share of Underground Cable) * log (Circuit Length)	0.299***
	[0.1065]		[0.1144]
Year trend	0.012***	Year trend	-0.009
	[0.0018]		[0.0127]
		Heteroscedasticity in idiosyncratic error variance	
		Constant	-3.527***
			[0.2829]
		log (Circuit Length)	0.047
			[0.0774]
		log (Circuit Length)^2	0.082**
			[0.0343]
Observations	945		

Note: The left-hand side of the table shows the estimates of the cost frontier (i.e., equation (4.1)) and the right-hand side contains the estimates of the variance specification for both the technical inefficiency and the idiosyncratic error (i.e., equations (4.2)-(4.3)). Standard errors in parentheses. ***, **, and * indicate statistical significance at 1%, 5% and 10% nominal level, respectively.

Table B.4: Cost frontier and technical efficiency estimates - Half Normal Distribution

Cost Frontier Estimates		**Variance estimates technical inefficiency & idiosyncratic shock**	
Variable	Coefficient	Variable	Coefficient
log (Customer Number)	0.334*	*Heteroscedasticity in technical inefficiency variance*	
	[0.1888]		
log (Ratcheted Max Demand)	0.244	Constant	-4.477***
	[0.1622]		[1.1165]
log (Circuit Length)	0.290**	log (Circuit Length)	-0.539*
	[0.1148]		[0.3041]
log (Circuit Length) * log (Customer Number)	0.103	log (Share of Underground Cable)	-2.163**
	[0.0774]		[1.0198]
log (Customer Number) * log (Ratcheted Max Demand)	-0.506***	log (Share of Underground Cable)^2	-0.375
	[0.1152]		[0.2464]
log (Circuit Length) * log (Ratcheted Max Demand)	0.307**	log (Share of Underground Cable) * log (Circuit Length)	-0.147
	[0.1289]		[0.1126]
Year trend	0.015***	Year trend	-0.052***
	[0.0025]		[0.0191]
		Heteroscedasticity in idiosyncratic error variance	
		Constant	-2.274***
			[0.0654]
		log (Circuit Length)	0.331***
			[0.0835]
		log (Circuit Length)^2	-0.099***
			[0.0316]
Observations	945		

Note: The left-hand side of the table shows the estimates of the cost frontier (i.e., equation (4.1)) and the right-hand side contains the estimates of the variance specification for both the technical inefficiency and the idiosyncratic error (i.e., equations (4.2)-(4.3)). Standard errors in parentheses. ***, **, and * indicate statistical significance at 1%, 5% and 10% nominal level, respectively.

Figure B.2: Relative technical efficiency for each Australian DNSPs assuming Exponential distribution for inefficiencies

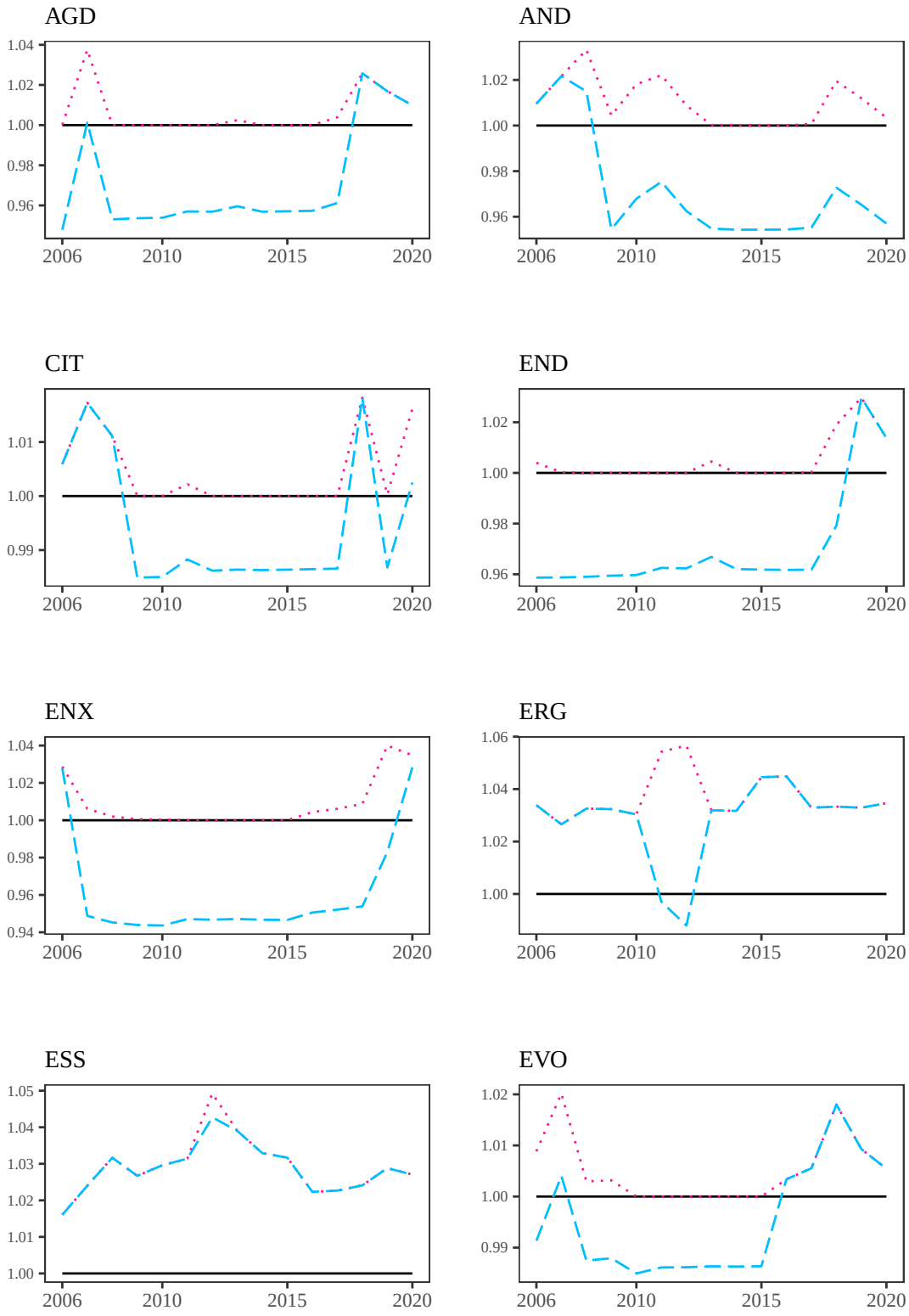

(Continued on next page)

Relative technical efficiency for each Australian DNSPs assuming Exponential distribution for inefficiencies (continued from previous page)

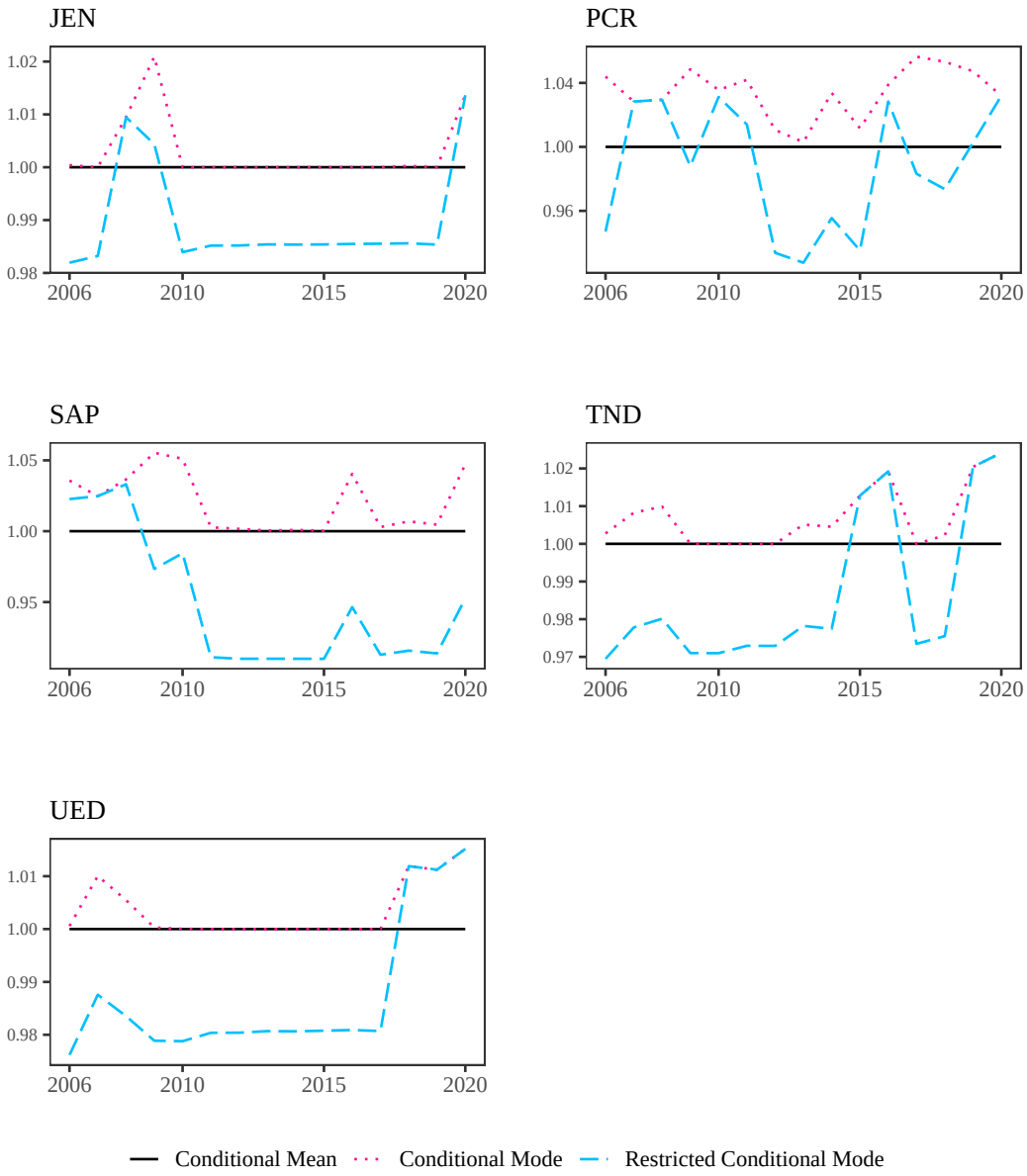

Figure B.3: Relative technical efficiency for each Australian DNSPs assuming Half Normal distribution for inefficiencies

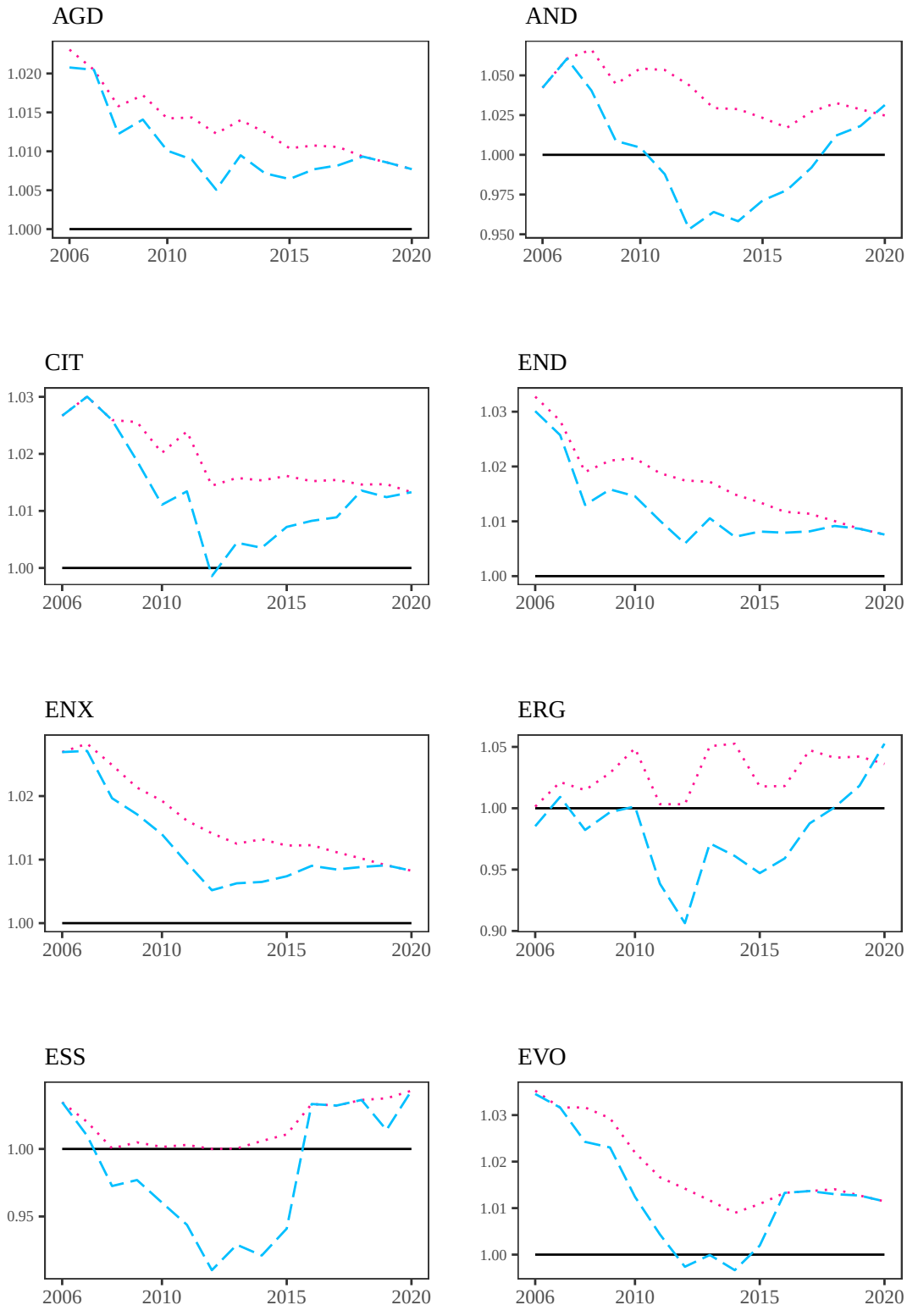

(Continued on next page)

Relative technical efficiency for each Australian DNSPs assuming Half Normal distribution for inefficiencies (continued from previous page)

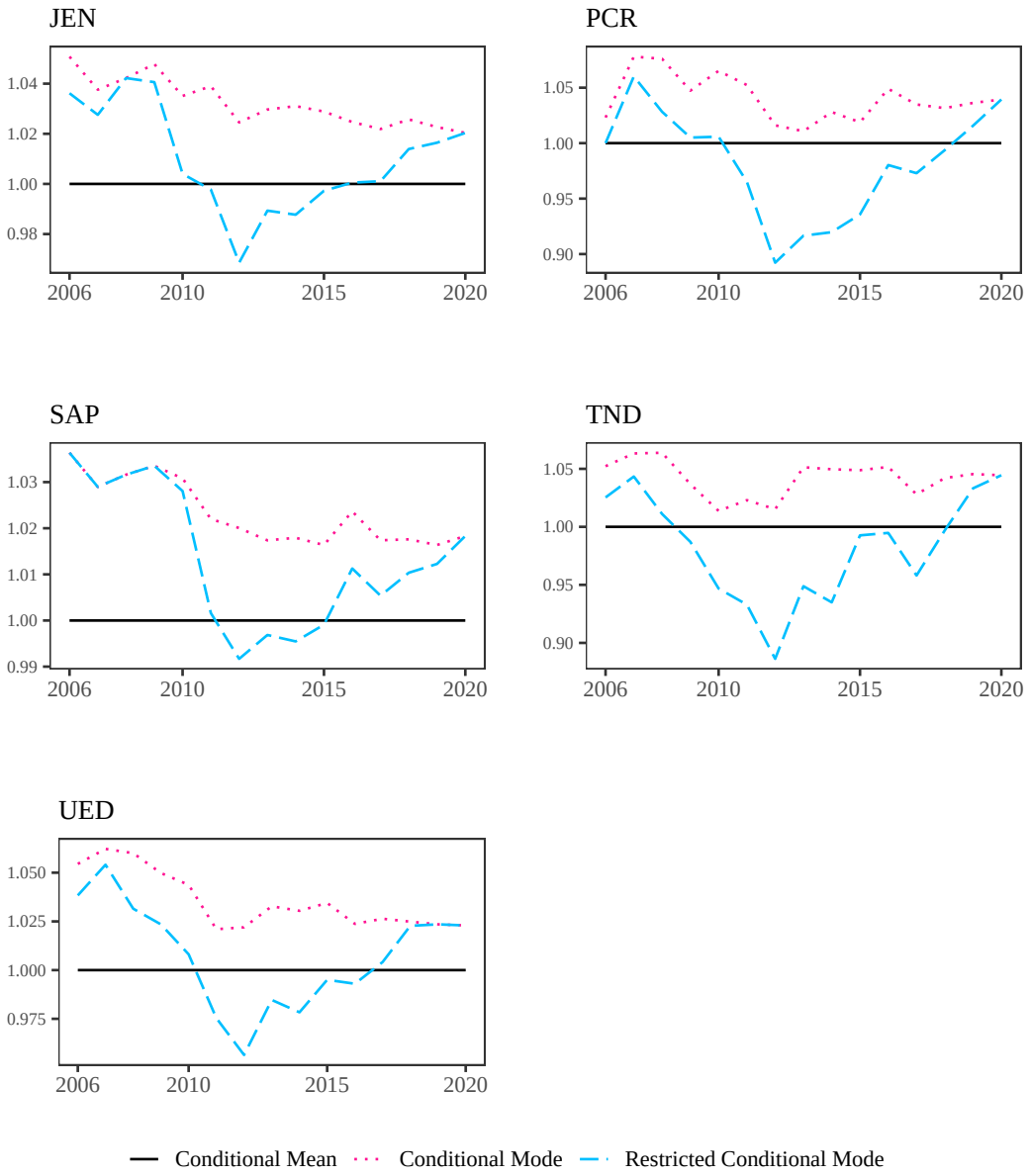

Table B.5: Efficiency Rank of DNSPs for Exponential Inefficiency

Rank	2006	2007	2008	2009	2010	2011	2012	2013	2014	2015	2016	2017	2018	2019	2020
1	CIT	CIT	CIT	ERG	ERG	ESS	ESS	ERG	ERG	ERG	AVO	AVO	AVO	AVO	AVO
2	ERG	ERG	ERG	ESS	ESS	PCR	ERG	ESS	ESS	ESS	ERG	ERG	AGD	AGD	AGD
3	ESS	ESS	ESS	JEN	PCR	ERG	AND	TND	TND	TND	ESS	ESS	CIT	END	END
4	AND	PCR	JEN	PCR	SAP	CIT	PCR	END	PCR	UED	TND	PCR	ERG	ERG	ERG
5	ENX	SAP	PCR	AVO	AND	AND	JEN	AGD	JEN	JEN	PCR	CIT	ESS	ESS	ESS
6	SAP	AND	SAP	SAP	UED	JEN	END	JEN	UED	CIT	SAP	AGD	UED	TND	JEN
7	AVO	AVO	AND	CIT	AVO	AVO	SAP	UED	AND	PCR	ENX	ENX	END	UED	PCR
8	JEN	AGD	AVO	UED	JEN	TND	CIT	AND	CIT	END	CIT	UED	PCR	PCR	TND
9	TND	UED	UED	AND	CIT	END	AVO	PCR	END	AND	JEN	AND	AND	ENX	UED
10	UED	TND	TND	TND	END	SAP	TND	CIT	AGD	ENX	UED	END	JEN	CIT	ENX
11	PCR	ENX	ENX	ENX	ENX	ENX	UED	SAP	ENX	SAP	AGD	JEN	TND	AND	CIT
12	END	JEN	END	END	TND	AGD	ENX	AVO	SAP	AVO	END	TND	ENX	JEN	SAP
13	AGD	END	AGD	AGD	AGD	UED	AGD	ENX	AVO	AGD	AND	SAP	SAP	SAP	AND

Table B.6: Efficiency Rank of DNSPs for Half Normal Inefficiency

Rank	2006	2007	2008	2009	2010	2011	2012	2013	2014	2015	2016	2017	2018	2019	2020
1	CIT	AVO	CIT	SAP	SAP	AGD	AGD	AGD	AGD	END	AVO	AVO	AGD	AVO	AVO
2	ENX	AGD	JEN	ENX	ENX	CIT	ENX	END	END	ENX	ESS	ESS	ESS	AGD	AGD
3	ESS	CIT	SAP	AVO	END	ENX	END	ENX	ENX	AGD	ENX	AGD	END	END	CIT
4	SAP	SAP	ENX	AGD	AGD	END	CIT	CIT	CIT	CIT	AGD	ENX	CIT	ENX	END
5	AND	AND	AVO	JEN	AVO	AVO	AVO	AVO	AVO	AVO	END	END	AVO	UED	ENX
6	AVO	ENX	AGD	CIT	CIT	SAP	SAP	SAP	SAP	SAP	CIT	CIT	ENX	CIT	ESS
7	END	END	END	END	UED	JEN	JEN	JEN	JEN	JEN	SAP	SAP	UED	JEN	JEN
8	AGD	UED	AND	UED	JEN	AND	AND	UED	UED	UED	JEN	UED	SAP	SAP	PCR
9	JEN	PCR	UED	AND	AND	UED	UED	ERG	ERG	TND	UED	JEN	JEN	TND	SAP
10	UED	JEN	PCR	PCR	PCR	PCR	PCR	AND	AND	AND	TND	AND	AND	AND	TND
11	TND	TND	TND	ERG	ERG	TND	TND	TND	TND	ERG	PCR	ERG	ERG	ERG	UED
12	PCR	ESS	ERG	TND	TND	ESS	ERG	PCR	PCR	PCR	AND	PCR	TND	PCR	ERG
13	ERG	ERG	ESS	ESS	ESS	ERG	ESS	ESS	ESS	ESS	ERG	TND	PCR	ESS	AND

Table B.7: Ranking of DNSP by efficiency– Half Normal distribution

DNSP	Minimum	Maximum	Median	Mean
AGD	1	8	2	2.87
ENX	2	6	3	3.4
AVO	1	6	5	3.6
CIT	1	6	4	4
END	1	7	4	4.2
SAP	1	9	6	5.47
JEN	2	10	7	7.27
UED	5	11	8	8.27
AND	5	13	10	9.13
ESS	2	13	13	9.53
PCR	8	13	11	10.87
TND	9	13	11	10.93
ERG	9	13	11	11.47

Table B.8: Ranking of DNSP by efficiency–Exponential distribution

DNSP	Minimum	Maximum	Median	Mean
ERG	1	4	2	2.13
ESS	1	5	3	2.8
PCR	2	11	5	5.67
AVO	1	13	7	6.13
CIT	1	11	7	6.13
JEN	3	12	6	7.33
AND	3	13	8	7.87
TND	3	12	9	7.93
UED	4	13	8	8.2
END	3	13	9	8.67
SAP	4	13	10	9
AGD	2	13	11	9.07
ENX	5	13	11	10.07

References

Abdul-Salam, Y. and E. Phimister (2017). Efficiency effects of access to information on small-scale agriculture: Empirical evidence from uganda using stochastic frontier and IRT models. *Journal of Agricultural Economics 68*(2), 494–517.

AER (2021). Annual benchmarking report. electricity distribution network service providers. In *Annual Benchmarking Report*. Australian Energy Regulator. https://www.aer.gov.au/system/files/Distribution

Andor, M. A., C. Parmeter, and S. Sommer (2019). Combining uncertainty with uncertainty to get certainty? efficiency analysis for regulation purposes. *European Journal of Operational Research 274*(1), 240–252.

Badunenko, O., D. J. Henderson, and S. C. Kumbhakar (2012). When, where and how to perform efficiency estimation. *Journal of the Royal Statistical Society Series A: Statistics in Society 175*(4), 863–892.

Belotti, F. and G. Ilardi (2018). Consistent inference in fixed-effects stochastic frontier models. *Journal of Econometrics 202*(2), 161–177.

Belotti, F., G. Ilardi, et al. (2014). sftfe: A stata command for fixed-effects stochastic frontier models estimation. In *Ital. Stata Users' Gr. Meet. 2014 (No. 05)*. Citeseer.

Caudill, S. B. and J. M. Ford (1993). Biases in frontier estimation due to heteroscedasticity. *Economics Letters 41*(1), 17–20.

Caudill, S. B., J. M. Ford, and D. M. Gropper (1995). Frontier estimation and firm-specific inefficiency measures in the presence of heteroscedasticity. *Journal of Business & Economic Statistics 13*(1), 105–111.

Chen, Y.-Y., P. Schmidt, and H.-J. Wang (2014). Consistent estimation of the fixed effects stochastic frontier model. *Journal of Econometrics 181*(2), 65–76.

Fenn, P., D. Vencappa, S. Diacon, P. Klumpes, and C. O'Brien (2008). Market structure and the efficiency of european insurance companies: A stochastic frontier analysis. *Journal of Banking & Finance 32*(1), 86–100.

Greene, W. (2005a). Fixed and random effects in stochastic frontier models. *Journal of Productivity Analysis 23*(1), 7–32.

Greene, W. (2005b). Reconsidering heterogeneity in panel data estimators of the stochastic frontier model. *Journal of Econometrics 126*(2), 269–303.

Honoré, B. E. and J. L. Powell (1994). Pairwise difference estimators of censored and truncated regression models. *Journal of Econometrics 64*(1-2), 241–278.

Horrace, W. C. (2005). On ranking and selection from independent truncated normal distributions. *Journal of Econometrics 126*(2), 335–354.

Horrace, W. C., H. Jung, and Y. Yang (2023, December). The conditional mode in parametric frontier models. *Journal of Productivity Analysis 60*(3), 333–343.

Jamasb, T. and M. Söderberg (2010). The effects of average norm model regulation: The case of electricity distribution in sweden. *Review of Industrial Organization 36*, 249–269.

Jondrow, J., C. Knox Lovell, I. S. Materov, and P. Schmidt (1982). On the estimation of technical inefficiency in the stochastic frontier production function model. *Journal of econometrics 19*(2-3), 233–238.

Kumbhakar, S. C., A. P. Horncastle, et al. (2015). *A practitioner's guide to stochastic frontier analysis using Stata*. Cambridge University Press.

Kumbhakar, S. C., G. Lien, and J. B. Hardaker (2014). Technical efficiency in competing panel data models: a study of norwegian grain farming. *Journal of Productivity Analysis 41*(2), 321–337.

Kumbhakar, S. C. and C. K. Lovell (2003). *Stochastic frontier analysis*. Cambridge university press.

Kumbhakar, S. C., C. F. Parmeter, and V. Zelenyuk (2020). *Stochastic Frontier Analysis: Foundations and Advances I*, pp. 1–40. Singapore: Springer Singapore.

Lawrence, D., T. Coelli, and J. Kain (2018). Economic benchmarking results for the australian energy regulator's 2019 dnsp. In *Annual Benchmarking Report*. Australian Regulator Energy.

Lee, B. L., C. Wilson, P. Simshauser, and E. Majiwa (2021). Deregulation, efficiency and policy determination: An analysis of australia's electricity distribution sector. *Energy Economics 98*, 105210.

Lovell, C. K. (2006). Frontier analysis in healthcare. *International journal of healthcare technology and management 7*(1-2), 5–14.

Manzur Quader, S. and M. Dietrich (2014). Corporate efficiency in the uk: a stochastic frontier analysis. *International Journal of Productivity and Performance Management 63*(8), 991–1011.

Nazarko, J. and E. Chodakowska (2017). Labour efficiency in construction industry in europe based on frontier methods: Data envelopment analysis and stochastic frontier analysis. *Journal of Civil Engineering and Management 23*(6), 787–795.

Piacenza, M. (2006). Regulatory contracts and cost efficiency: Stochastic frontier evidence from the italian local public transport. *Journal of Productivity Analysis 25*(3), 257–277.

Price, J. I., S. Renzetti, D. Dupont, W. Adamowicz, and M. B. Emelko (2017). Production costs, inefficiency, and source water quality: A stochastic cost frontier analysis of canadian water utilities. *Land Economics 93*(1), 1–11.

Roberts, S. (2018). Consultation on draft decision paper on forecasting productivity growth for electricity distributors. In *Annual Benchmarking Report*. Australian Energy Regulator.

Söderberg, M. (2008). Four essays on efficiency in swedish electricity distribution. *PhD Thesis*.

Stone, M. (2002). How not to measure the efficiency of public services (and how one might). *Journal of the Royal Statistical Society Series A: Statistics in Society 165*(3), 405–434.

Tsionas, M. G. (2017). "when, where, and how" of efficiency estimation: improved procedures for stochastic frontier modeling. *Journal of the American Statistical Association 112*(519), 948–965.

Wang, H.-J. (2002). Heteroscedasticity and non-monotonic efficiency effects of a stochastic frontier model. *Journal of Productivity Analysis 18*(3), 241–253.

Wang, H.-J. and C.-W. Ho (2010). Estimating fixed-effect panel stochastic frontier models by model transformation. *Journal of Econometrics 157*(2), 286–296.

Wang, W. S. and P. Schmidt (2009). On the distribution of estimated technical efficiency in stochastic frontier models. *Journal of Econometrics 148*(1), 36–45.

Zeebari, Z., K. Månsson, P. Sjölander, and M. Söderberg (2021). Regularized conditional estimators of unit inefficiency in stochastic frontier analysis, with application to electricity distribution market. Technical report, The Ratio Institute.

Zeebari, Z., K. Månsson, P. Sjölander, and M. Söderberg (2023). Regularized conditional estimators of unit inefficiency in stochastic frontier analysis, with application to electricity distribution market. *Journal of Productivity Analysis 59*(1), 79–97.